

Chapter 2

Radiation of Electromagnetic Waves by Impedance Vibrators in Free Space and Material Medium

2.1 Asymptotic Solution of Integral Equations for Vibrator Current in Free Space

Let us rewrite (1.22) ($z_i(s) = \text{const}, \varepsilon_1 = \mu_1 = 1$), using the approximate kernel (1.21), the quasi-unidimensional analog of the exact integral equation with the kernel (1.20), as

$$\left(\frac{d^2}{ds^2} + k^2\right) \int_{-L}^L J(s') \frac{e^{-ikR(s,s')}}{R(s,s')} ds' = -i\omega E_{0s}(s) + i\omega z_i J(s), \quad (2.1)$$

where $R(s,s') = \sqrt{(s-s')^2 + r^2}$. It is obvious that $F_0[s, J(s)] \equiv 0$. We isolate the logarithmic kernel singularity as in (1.45):

$$\int_{-L}^L J(s') \frac{e^{-ikR(s,s')}}{R(s,s')} ds' = \Omega(s)J(s) + \int_{-L}^L \frac{J(s')e^{-ikR(s,s')} - J(s)}{R(s,s')} ds'. \quad (2.2)$$

Here

$$\Omega(s) = \int_{-L}^L \frac{ds'}{\sqrt{(s-s')^2 + r^2}} = \Omega + \gamma(s), \quad (2.3)$$

and

$$\gamma(s) = \ln \frac{\left[(L+s) + \sqrt{(L+s)^2 + r^2}\right] \left[(L-s) + \sqrt{(L-s)^2 + r^2}\right]}{4L^2}$$

is a function equal to zero in the vibrator center which attains its largest value on the vibrator's ends, where the current equals zero. In view of boundary conditions

(1.18), $\Omega = 2 \ln(2L/r)$ is a large parameter. Then, with (2.3), (2.1) is transformed into the following integrodifferential equation:

$$\frac{d^2 J(s)}{ds^2} + k^2 J(s) = \alpha \{ i\omega E_{0s}(s) + F[s, J(s)] - i\omega z_i J(s) \}, \quad (2.4)$$

where $\alpha = 1/(2 \ln[r/(2L)])$ is a natural small parameter ($|\alpha| \ll 1$) and

$$\begin{aligned} F[s, J(s)] = & -\frac{dJ(s')}{ds'} \frac{e^{-ikR(s,s')}}{R(s,s')} \Big|_{-L}^L + \left[\frac{d^2 J(s)}{ds^2} + k^2 J(s) \right] \gamma(s) \\ & + \int_{-L}^L \frac{\left[\frac{d^2 J(s')}{ds'^2} + k^2 J(s') \right] e^{-ikR(s,s')} - \left[\frac{d^2 J(s)}{ds^2} + k^2 J(s) \right]}{R(s,s')} ds' \end{aligned} \quad (2.5)$$

is the vibrator's self-field in free space.

Let us apply the asymptotic averaging method outlined in Sect. 1.5 to obtain the approximate analytical solution of (2.4). To reduce (2.4) to the standard form (1.62) with small parameter in accordance with the method of arbitrary constants variation, we change variables and get

$$\begin{aligned} J(s) &= A(s) \cos ks + B(s) \sin ks, \\ \frac{dJ(s)}{ds} &= -A(s)k \sin ks + B(s)k \cos ks, \quad \left(\frac{dA(s)}{ds} \cos ks + \frac{dB(s)}{ds} \sin ks = 0 \right), \\ \frac{d^2 J(s)}{ds^2} + k^2 J(s) &= -\frac{dA(s)}{ds} \sin ks + \frac{dB(s)}{ds} \cos ks \end{aligned} \quad (2.6)$$

where $A(s)$ and $B(s)$ are the new unknown functions. Then (2.4) is converted into the following system of the integrodifferential equations:

$$\begin{aligned} \frac{dA(s)}{ds} &= -\frac{\alpha}{k} \left\{ i\omega E_{0s}(s) + F \left[s, A(s), \frac{dA(s)}{ds}, B(s), \frac{dB(s)}{ds} \right] \right. \\ &\quad \left. - i\omega z_i [A(s) \cos ks + B(s) \sin ks] \right\} \sin ks, \\ \frac{dB(s)}{ds} &= +\frac{\alpha}{k} \left\{ i\omega E_{0s}(s) + F \left[s, A(s), \frac{dA(s)}{ds}, B(s), \frac{dB(s)}{ds} \right] \right. \\ &\quad \left. - i\omega z_i [A(s) \cos ks + B(s) \sin ks] \right\} \cos ks. \end{aligned} \quad (2.7)$$

The obtained equations are equivalent to (2.4) and represent the standard system of integrodifferential equations (1.62), unresolved relative to the derivative. The right-hand sides in (2.7) are proportional to the small parameter α , so the functions $A(s)$ and $B(s)$ on the right-hand sides of (2.7) are slowly changing functions, and the averaging asymptotic method can be used for its solution. Then putting into correspondence the simplified system (1.63) with $dA(s)/ds = 0$ and $dB(s)/ds = 0$ on the

right-hand sides and the system (2.7), after performing partial averaging over s explicitly (here the term “partial” means that the averaging operator (1.54) acts on all summands except those containing $E_{0s}(s)$, which is possible ([22] in Chap. 1) for system (2.7)), we obtain the equations of first approximation

$$\begin{aligned}\frac{d\bar{A}(s)}{ds} &= -\alpha \left\{ \frac{i\omega}{k} E_{0s}(s) + \bar{F}[s, \bar{A}(s), \bar{B}(s)] \right\} \sin ks + \chi \bar{B}(s), \\ \frac{d\bar{B}(s)}{ds} &= +\alpha \left\{ \frac{i\omega}{k} E_{0s}(s) + \bar{F}[s, \bar{A}(s), \bar{B}(s)] \right\} \cos ks - \chi \bar{A}(s),\end{aligned}\quad (2.8)$$

where $\chi = \alpha(i\omega/2k)z_i$, and

$$\bar{F}[s, \bar{A}(s), \bar{B}(s)] = [\bar{A}(s') \sin ks' - \bar{B}(s') \cos ks'] \frac{e^{-ikR(s,s')}}{R(s,s')} \Big|_{-L}^L \quad (2.9)$$

is the self-field of the vibrator (2.5), averaged along its length.

We shall obtain the solution of the system (2.8) in the form [1]

$$\begin{aligned}\bar{A}(s) &= C_1(s) \cos \chi s + C_2(s) \sin \chi s, \\ \bar{B}(s) &= -C_1(s) \sin \chi s + C_2(s) \cos \chi s,\end{aligned}\quad (2.10)$$

transforming (2.8) into

$$\begin{aligned}\frac{dC_1(s)}{ds} &= -\alpha \left\{ \frac{i\omega}{k} E_{0s}(s) + \bar{F}[s, C_1, C_2] \right\} \sin(k + \chi)s, \\ \frac{dC_2(s)}{ds} &= +\alpha \left\{ \frac{i\omega}{k} E_{0s}(s) + \bar{F}[s, C_1, C_2] \right\} \cos(k + \chi)s.\end{aligned}\quad (2.11)$$

Then we obtain $C_1(s)$, $C_2(s)$ from (2.11), and $\bar{A}(s)$, $\bar{B}(s)$ from (2.10), and use these functions as the approximating functions for the current in (2.6). As a result, we obtain the most general asymptotic expression in the parameter α for the current in the thin impedance vibrator with arbitrary excitation:

$$\begin{aligned}J(s) &= \bar{A}(-L) \cos(\tilde{k}s + \chi L) + \bar{B}(-L) \sin(\tilde{k}s + \chi L) \\ &\quad + \alpha \int_{-L}^s \left\{ \frac{i\omega}{k} E_{0s}(s') + \bar{F}[s', \bar{A}, \bar{B}] \right\} \sin \tilde{k}(s - s') ds',\end{aligned}\quad (2.12)$$

where $\tilde{k} = k + \chi = k + i(\alpha/r)\bar{Z}_S$.

To find the constants $\bar{A}(\pm L)$ and $\bar{B}(\pm L)$, it is necessary to use the boundary conditions (1.18) and the conditions of symmetry ([11] in Chap. 1) related to the method of vibrator excitation. If $E_{0s}(s) = E_{0s}^s(s)$, then $J(s) = J(-s) = J^s(s)$ and $\bar{A}(-L) = \bar{A}(+L)$, $\bar{B}(-L) = -\bar{B}(+L)$; if $E_{0s}(s) = E_{0s}^a(s)$, then $J(s) = -J(-s) = J^a(s)$ and $\bar{A}(-L) = -\bar{A}(+L)$, $\bar{B}(-L) = \bar{B}(+L)$. Then for symmetric (index “s”) and antisymmetric (index “a”) current components, we finally obtain, for arbitrary excitation $E_{0s}(s) = E_{0s}^s(s) + E_{0s}^a(s)$,

$$J(s) = J^s(s) + J^a(s) = \alpha \frac{i\omega}{k} \left\{ \int_{-L}^s E_{0s}(s') \sin \tilde{k}(s - s') ds' - \frac{\sin \tilde{k}(L + s) + \alpha P^s[kr, \tilde{k}(L + s)]}{\sin 2\tilde{k}L + \alpha P^s(kr, 2\tilde{k}L)} \int_{-L}^L E_{0s}^s(s') \sin \tilde{k}(L - s') ds' - \frac{\sin \tilde{k}(L + s) + \alpha P^a[kr, \tilde{k}(L + s)]}{\sin 2\tilde{k}L + \alpha P^a(kr, 2\tilde{k}L)} \int_{-L}^L E_{0s}^a(s') \sin \tilde{k}(L - s') ds' \right\}, \quad (2.13)$$

where P^s and P^a are the vibrator self-field functions, given by

$$P^s[kr, \tilde{k}(L + s)] = \int_{-L}^s \left[\frac{e^{-ikR(s', -L)}}{R(s', -L)} + \frac{e^{-ikR(s', L)}}{R(s', L)} \right] \sin \tilde{k}(s - s') ds' \Big|_{s=L} \quad (2.14a)$$

$$= P^s(kr, 2\tilde{k}L),$$

$$P^a[kr, \tilde{k}(L + s)] = \int_{-L}^s \left[\frac{e^{-ikR(s', -L)}}{R(s', -L)} - \frac{e^{-ikR(s', L)}}{R(s', L)} \right] \sin \tilde{k}(s - s') ds' \Big|_{s=L} \quad (2.14b)$$

$$= P^a(kr, 2\tilde{k}L).$$

2.2 Vibrator Excitation in the Center by Concentrated EMF

To validate the accuracy and to find the limits of applicability of (2.13), we shall discuss the classical problem of vibrator excitation in the geometrical center by lump EMF with amplitude V_0 . The mathematical model of excitation may be represented as

$$E_{0s}(s) = E_{0s}^s(s) = V_0 \delta(s - 0), \quad (2.15)$$

where $\delta(s - 0) = \delta(s)$ is Dirac's delta function. Then the expression for the current has the form

$$J(s) = -\alpha V_0 \left(\frac{i\omega}{2\tilde{k}} \right) \frac{\sin \tilde{k}(L - |s|) + \alpha P_\delta^s(kr, \tilde{k}s)}{\cos \tilde{k}L + \alpha P_L^s(kr, \tilde{k}L)}. \quad (2.16)$$

Here $P_\delta^s(kr, \tilde{k}s) = P^s[kr, \tilde{k}(L + s)] - (\sin \tilde{k}s + \sin \tilde{k}|s|)P_L^s(kr, \tilde{k}L)$, $P^s[kr, \tilde{k}(L + s)]$ is defined by (2.14a), and $P_L^s(kr, \tilde{k}L) = \int_{-L}^L (e^{-ikR(s,L)}/R(s,L)) \cos \tilde{k}s ds$.

It is possible to obtain $P_\delta^s(kr, \tilde{k}s)$ and $P_L^s(kr, \tilde{k}L)$ in explicit form by the technique of generalized integral functions (see Appendix C). Here we give an expression for $P_L^s(kr, \tilde{k}L)$:

$$\begin{aligned} P_L^s(kr, \tilde{k}L) = & \cos \tilde{k}L \left\{ 2 \ln 2 - \gamma(L) - \frac{1}{2} [\text{Cin}(2\tilde{k}L + 2kL) + \text{Cin}(2\tilde{k}L - 2kL)] \right. \\ & - \frac{i}{2} [\text{Si}(2\tilde{k}L + 2kL) - \text{Si}(2\tilde{k}L - 2kL)] \Big\} \\ & + \sin \tilde{k}L \left\{ \frac{1}{2} [\text{Si}(2\tilde{k}L + 2kL) + \text{Si}(2\tilde{k}L - 2kL)] \right. \\ & \left. - \frac{i}{2} [\text{Cin}(2\tilde{k}L + 2kL) - \text{Cin}(2\tilde{k}L - 2kL)] \right\}, \end{aligned} \quad (2.17)$$

where $\text{Si}(x)$ and $\text{Cin}(x)$ are the integral sine and cosine of the complex argument.

Expression (2.16), in contrast to the solution of the integrodifferential equation (2.4) for the vibrator current by the small parameter method, is given in [2] as

(a) For a tuned vibrator ($\tilde{k}L = n(\pi/2)$, where n is the integer),

$$J_0(s) = C_1 \cos \tilde{k}s + C_2 \sin \tilde{k}s, \quad (2.18a)$$

(b) For an untuned vibrator ($\tilde{k}L \neq n(\pi/2)$),

$$\begin{aligned} J(s) = \alpha J_1(s) = & -\alpha \frac{i\omega/\tilde{k}}{\sin 2\tilde{k}L} \left\{ \sin \tilde{k}(L - s) \int_{-L}^s E_{0s}(s') \sin \tilde{k}(L + s') ds' \right. \\ & \left. + \sin \tilde{k}(L + s) \int_s^L E_{0s}(s') \sin \tilde{k}(L - s') ds' \right\}, \end{aligned} \quad (2.18b)$$

or after substituting $E_{0s}(s) = V_0 \delta(s)$,

$$J(s) = -\alpha V_0 \frac{i\omega}{2\tilde{k}} \frac{\sin \tilde{k}(L - |s|)}{\cos \tilde{k}L}, \quad (2.18c)$$

where

$$\tilde{k} = k \sqrt{\frac{1 + i\alpha\omega z_i}{k^2}} = k \sqrt{\frac{1 + i2\alpha\bar{Z}_S}{(kr)}} \Big|_{|i2\alpha\bar{Z}_S/(kr)| \ll 1} \approx k + i \frac{\alpha}{r} \bar{Z}_S = \tilde{k}. \quad (2.19)$$

Solution of (2.4) by the iterations method (see Sect. 1.4.2) for the current in the zeroth and first approximations (with accuracy α^2 inclusive) has the form

$$J_0(s) = -\alpha V_0 \frac{i\omega}{2k} \frac{\sin k(L - |s|)}{\cos kL}, \quad (2.20a)$$

$$J_1(s) = -\alpha V_0 \frac{i\omega}{2k} \frac{\sin k(L - |s|) + \alpha F_1(kr, ks, z_i)}{\cos kL + \alpha F(kr, kL, z_i)}. \quad (2.20b)$$

In addition to the above-mentioned solutions, King and Wu have obtained the so-called trinomial formula for the current on a vibrator centrally excited by the δ -generator [3, 4],

$$J(s) = -\alpha_K V_0 \frac{i\omega}{2\tilde{k}} \frac{\sin \tilde{k}(L - |s|) + F_{K1}(\cos \tilde{k}s - \cos \tilde{k}L) + F_{K2}(\cos \frac{ks}{2} - \cos \frac{kL}{2})}{\cos \tilde{k}L}, \quad (2.21)$$

with \tilde{k} defined in (2.19) and

$$\alpha_K = \frac{1}{\Omega_K}, \quad \Omega_K = \begin{cases} \frac{|\Omega_K(0)|}{\sin kL}, & kL \leq \pi/2, \\ |\Omega_K(\frac{L-\pi}{4})|, & kL \geq \pi/2, \end{cases} \quad (2.22a)$$

$$\Omega_K(s) = \int_{-L}^L \frac{e^{-ikR(s,s')}}{R(s,s')} \sin k(L - |s'|) ds'. \quad (2.22b)$$

Coefficients F_{K1} and F_{K2} have been found approximately by transforming (2.1) into the Hallen linearized equation (1.42) using its kernel properties. It should be noted that (2.21) coincides with (2.18c) when $F_{K1} = 0$ and $F_{K2} = 0$.

Thus, the solution of integrodifferential equation (2.1) by the averaging method is given by (2.13), valid (in contrast to the solution by the small parameter method) both for tuned ($\sin 2kL = 0$) and untuned ($\sin 2kL \neq 0$) vibrators under arbitrary excitation. The solution of (2.1) by the iterations method requires that the impressed sources field be specified at the initial stage of problem solution. What is more, the distributed vibrator impedance begins to exhibit itself, as follows from (2.20) (in contrast to the solutions by the averaging and the small parameter methods), in the first and succeeding approximations in the small parameter. And finally, the

King–Wu trinomial formula requires different current representations for the tuned and untuned vibrators as in the small parameter method.

The true current distribution (2.16) allows one to calculate the electrodynamic characteristics of the impedance vibrator. Thus, we may obtain the following expression for the vibrator input impedance at the feed point $Z_{\text{in}} = R_{\text{in}} + iX_{\text{in}}$ (or the input admittance $Y_{\text{in}} = G_{\text{in}} + iB_{\text{in}} = 1/Z_{\text{in}}$):

$$Z_{\text{in}}[\text{ohm}] = \frac{V_0}{J(0)} = \left(\frac{60i\tilde{k}}{\alpha k} \right) \frac{\cos \tilde{k}L + \alpha P_{\text{L}}^s(kr, \tilde{k}L)}{\sin \tilde{k}L + \alpha P_{\delta\text{L}}(kr, \tilde{k}L)}, \quad (2.23)$$

where

$$\begin{aligned} P_{\delta\text{L}}(kr, \tilde{k}L) &= \int_{-L}^L \frac{e^{-ikR(s,L)}}{R(s,L)} \sin \tilde{k}|s| ds \\ &= \sin \tilde{k}L \left\{ -\gamma(L) + \frac{1}{2} [\text{Cin}(2\tilde{k}L + 2kL) \right. \\ &\quad \left. - \text{Cin}(2\tilde{k}L - 2kL)] - \text{Cin}(\tilde{k}L + kL) + \text{Cin}(\tilde{k}L - kL) \right. \\ &\quad \left. + \frac{i}{2} [\text{Si}(2\tilde{k}L + 2kL) - \text{Si}(2\tilde{k}L - 2kL)] - i[\text{Si}(\tilde{k}L + kL) - \text{Si}(\tilde{k}L - kL)] \right\} \\ &\quad + \cos \tilde{k}L \left\{ \frac{1}{2} [\text{Si}(2\tilde{k}L + 2kL) + \text{Si}(2\tilde{k}L - 2kL)] - \text{Si}(\tilde{k}L + kL) - \text{Si}(\tilde{k}L - kL) \right. \\ &\quad \left. - \frac{i}{2} [\text{Cin}(2\tilde{k}L + 2kL) + \text{Cin}(2\tilde{k}L - 2kL)] + i[\text{Cin}(\tilde{k}L + kL) + \text{Cin}(\tilde{k}L - kL)] \right\}. \end{aligned} \quad (2.24)$$

Then the voltage standing wave ratio (VSWR) in the feeder line with characteristic impedance W equals

$$\text{VSWR} = \frac{1 + |S_{11}|}{1 - |S_{11}|}, \quad S_{11} = \frac{Z_{\text{in}} - W}{Z_{\text{in}} + W}, \quad (2.25)$$

where S_{11} is the reflection coefficient in the feeder.

Let us present some numerical results. Figures 2.1–2.5 show the current amplitude–phase distributions $J(s) = |J(s)|e^{i\arg J(s)}$ in thin ($r/\lambda = 0.007022$) perfectly conducting vibrators with different electrical lengths, calculated with (2.16), in comparison with the experimental data from [5]. As can be seen, the trend of theoretical curves follows that of experimental results quite satisfactorily, with some differences in the absolute values. Such differences are also present in the vibrator input characteristics $Y_{\text{in}} = f(2L/\lambda)$ and $|S_{11}| = f(kL)$, calculated by (2.23) and (2.25) and shown in Figs. 2.6 and 2.7. In Fig. 2.7 the theoretical curves corresponding to the King–Middleton solution of Hallen’s equation by the iterations method in the second approximation ([11, 12] in Chap. 1) are also plotted, namely

Fig. 2.1 The current amplitude–phase distribution on a perfectly conducting vibrator ($r/\lambda = 0.007022$ and $2L/\lambda = 0.5$): 1 the calculation (2.16); 2 the experimental data [5]

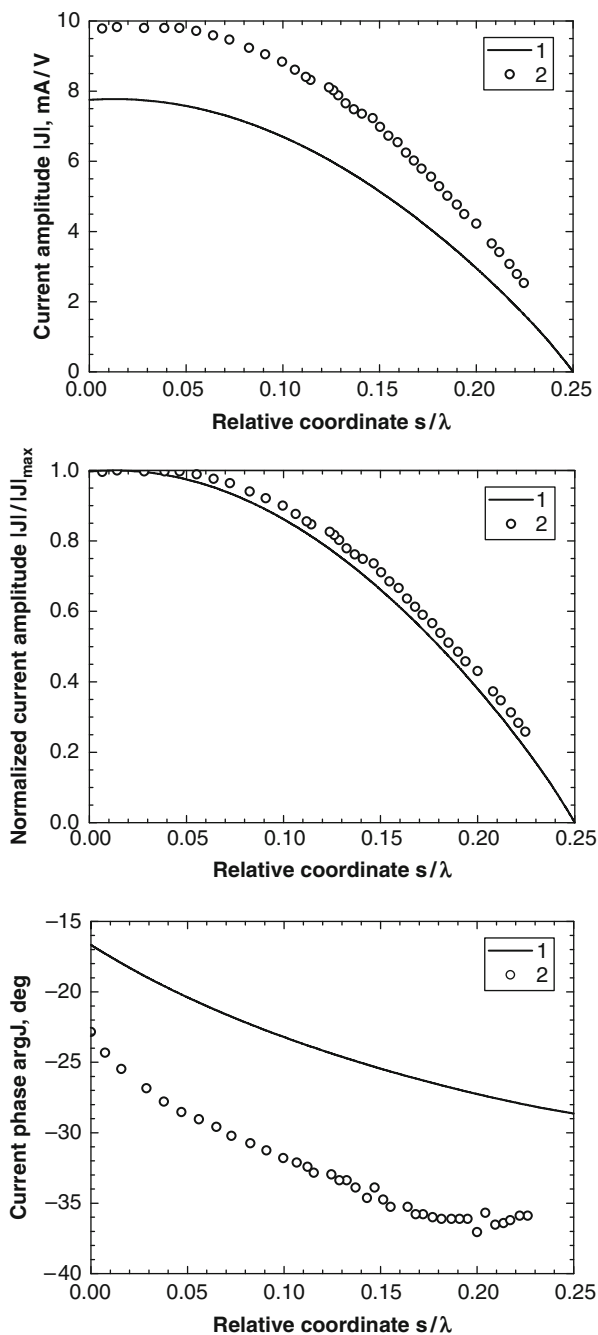


Fig. 2.2 The current amplitude–phase distribution on a perfectly conducting vibrator ($r/\lambda = 0.007022$ and $2L/\lambda = 0.75$): 1 the calculation (2.16); 2 the experimental data [5]

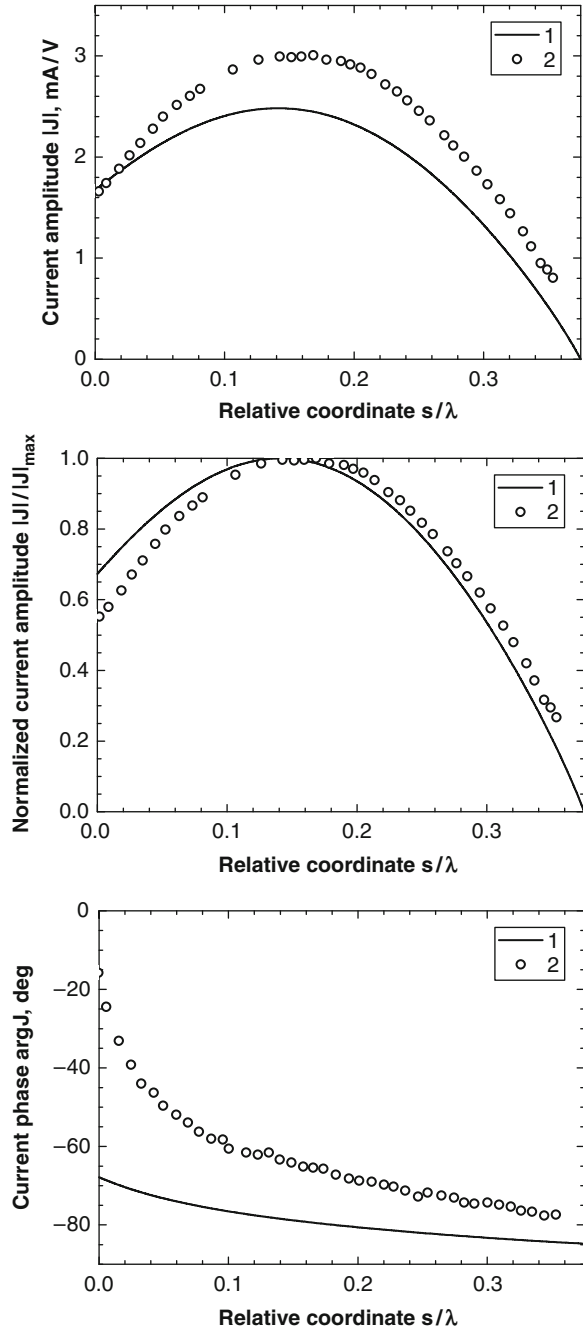


Fig. 2.3 The current amplitude–phase distribution on a perfectly conducting vibrator ($r/\lambda = 0.007022$ and $2L/\lambda = 1.0$): 1 the calculation (2.16); 2 the experimental data [5]

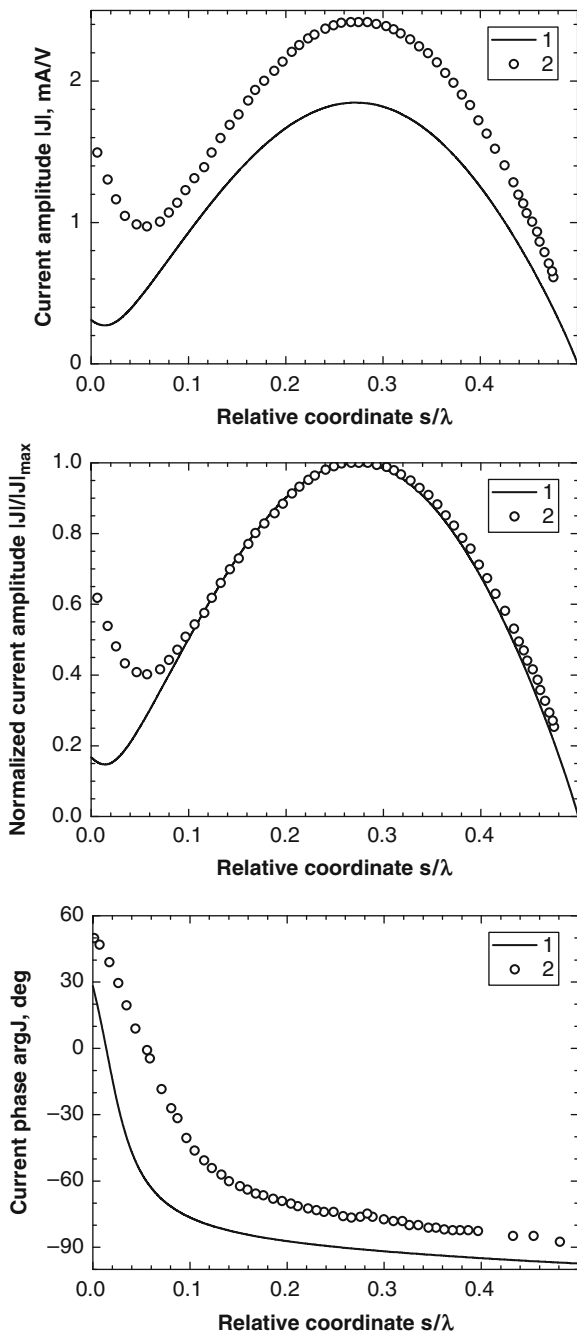


Fig. 2.4 The current amplitude-phase distribution on a perfectly conducting vibrator ($r/\lambda = 0.007022$ and $2L/\lambda = 1.25$): 1 the calculation (2.16); 2 the experimental data [5]

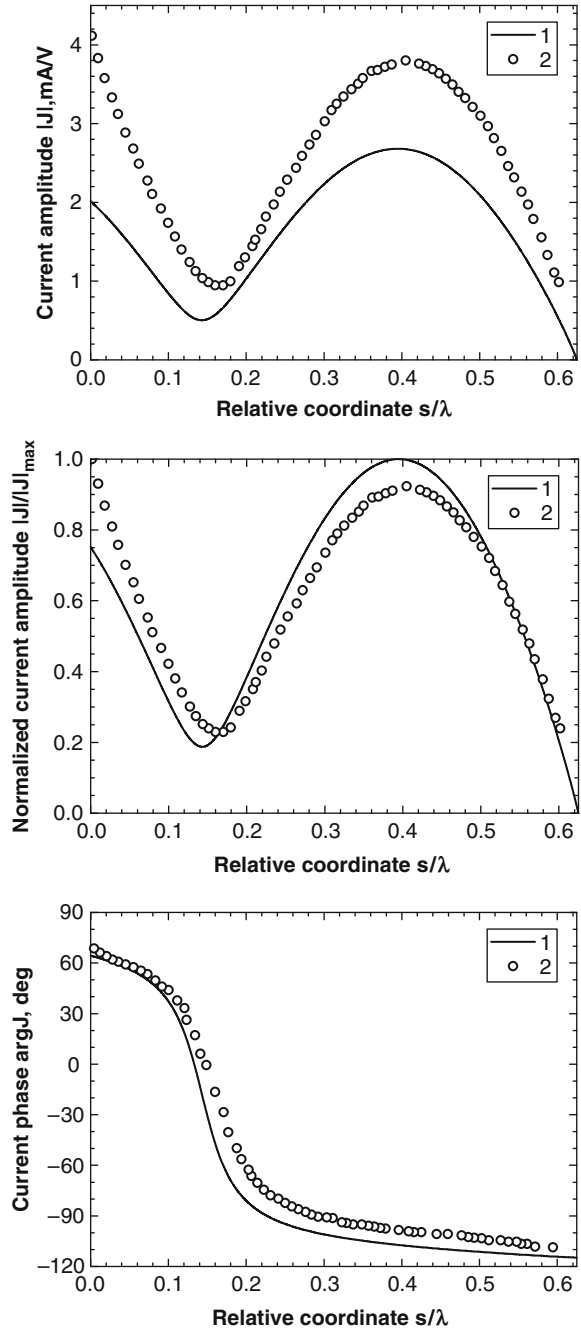
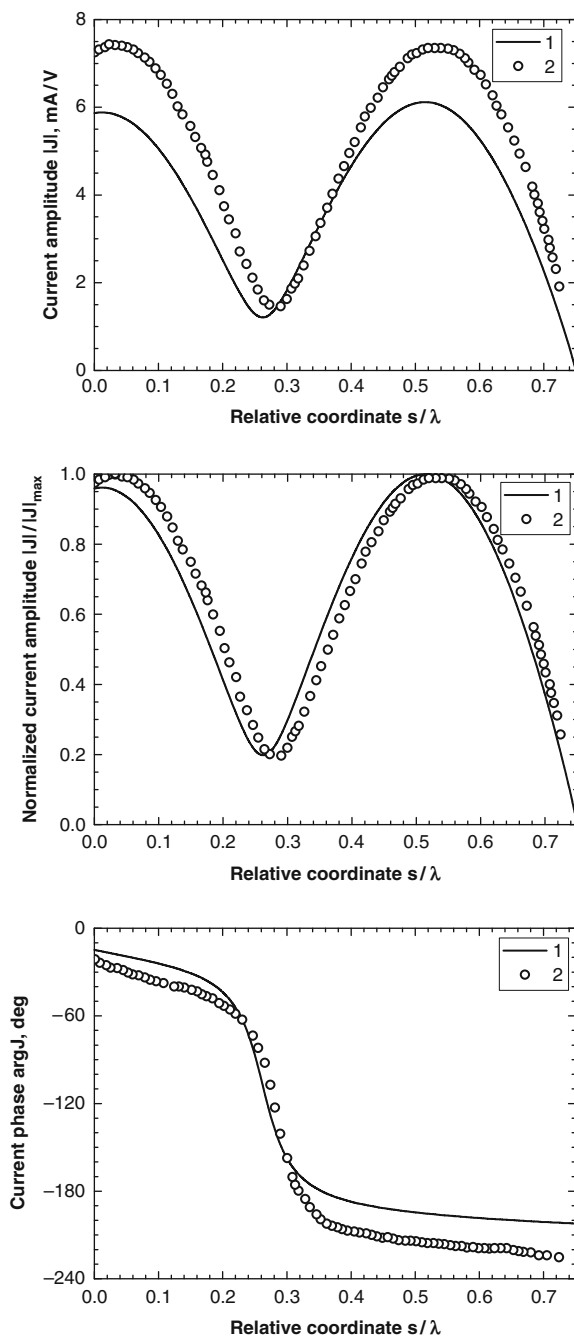


Fig. 2.5 The current amplitude–phase distribution on a perfectly conducting vibrator ($r/\lambda = 0.007022$ and $2L/\lambda = 1.5$): 1 the calculation (2.16); 2 the experimental data [5]



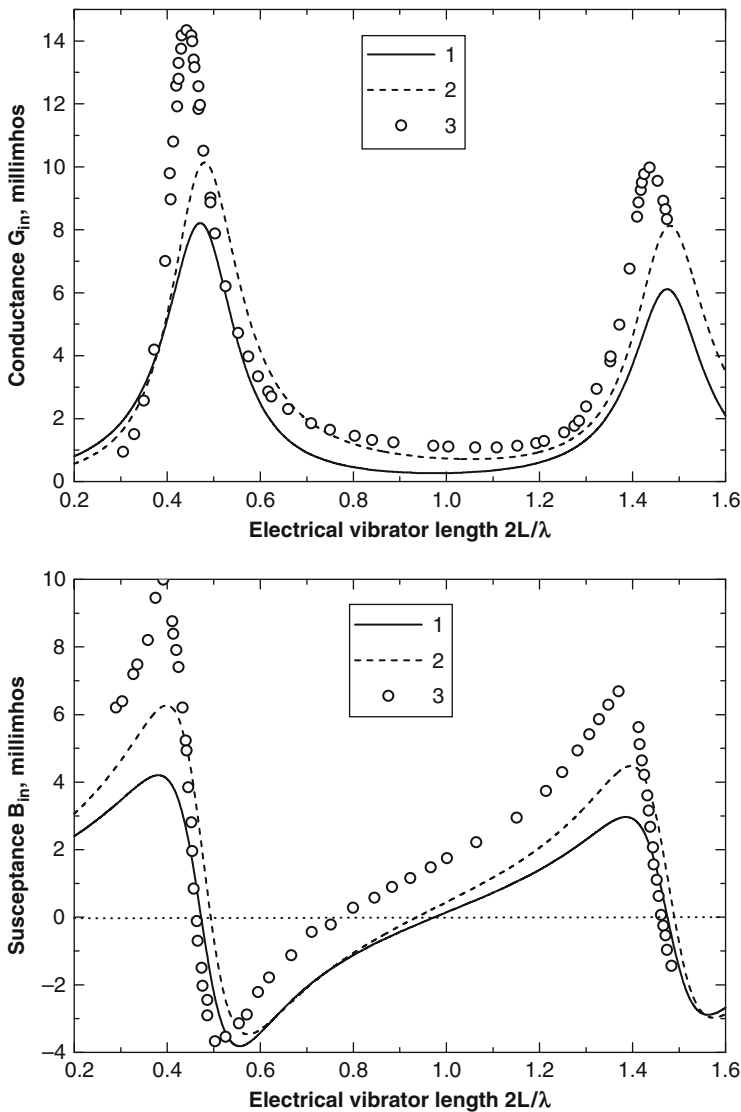


Fig. 2.6 The input admittance of a perfectly conducting vibrator versus electrical length ($r/\lambda = 0.007022$): 1 the calculation (2.23); 2 the calculation (2.27); 3 the experimental data [5]

$$Y_{in2}^K [\text{millimhos}] = \frac{i\alpha_K}{60} \frac{\sin kL + \alpha_K F_{1s}(kr, kL) + \alpha_K^2 F_{2s}(kr, kL)}{\cos kL + \alpha_K F_{1l}(kr, kL) + \alpha_K^2 F_{2l}(kr, kL)}, \quad (2.26)$$

where α_K is defined by (2.22).

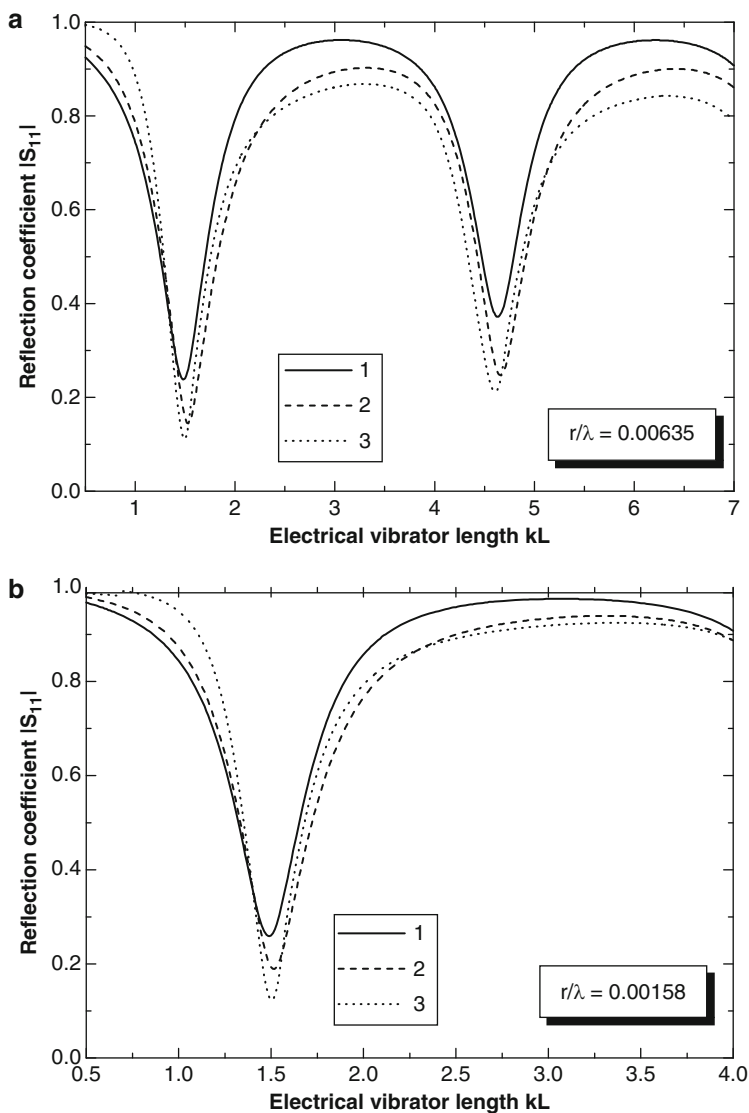


Fig. 2.7 The reflection coefficient in the feeder with $W = 75$ ohm versus electrical length of a perfectly conducting vibrator: 1 the calculation (2.23); 2 the calculation (2.27); 3 the calculation (2.26)

An analogous situation is observed for the input characteristics of impedance vibrators. The plots of input admittance for two different surface impedances are represented in Figs. 2.8 and 2.9: (1) a metallic conductor (radius $r_i = 0.3175$ cm)

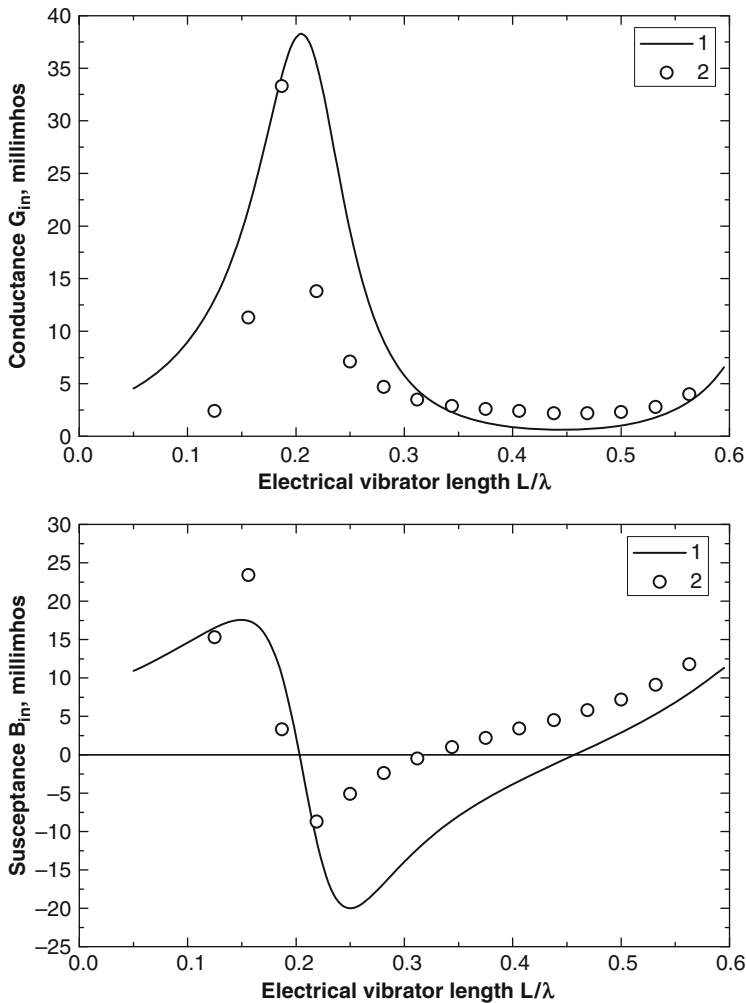


Fig. 2.8 Input admittance of a metallic conductor of radius $r_i = 0.3175$ cm, covered by a dielectric ($\varepsilon = 9.0$) shell with radius $r = 0.635$ cm versus electrical length at 600 MHz: 1 the calculation (2.23); 2 the experimental data [6]

covered by a dielectric ($\varepsilon = 9.0$) shell (radius $r = 0.635$ cm), where Fig. 2.8 shows experimental data from [6]; (2) a metallic conductor (radius $r_i = 0.5175$ cm) covered by a ferrite ($\mu = 4.7$) shell (radius $r = 0.6$ cm), where Fig. 2.9 shows experimental data from [7].

Differences among the theoretical curves obtained from solution of the integral equation by the averaging method, the experimental data, and the graphs plotted by

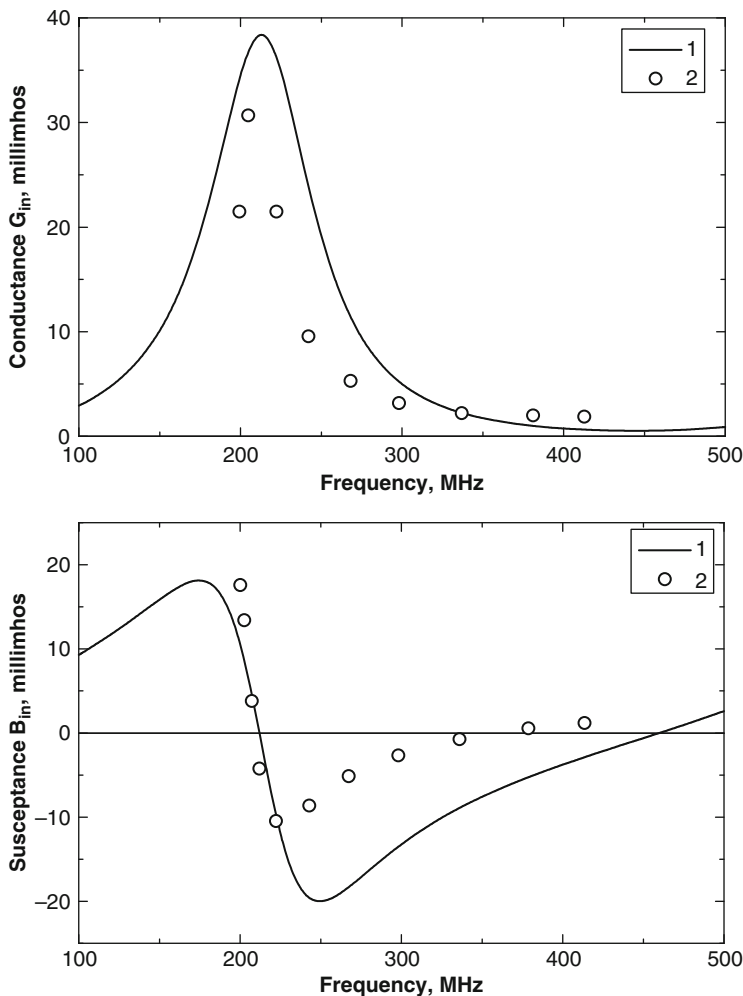


Fig. 2.9 Input admittance of a metallic conductor of radius $r_i = 0.5175$ cm covered by a ferrite ($\mu = 4.7$) shell with radius $r = 0.6$ cm versus frequency at $L = 30$ cm: 1 the calculation (2.23); 2 the experimental data [7]

higher approximations of the iterations method may be explained by errors in averaging of the self-field of the vibrator (2.5). However, the resonant characteristics of the vibrators ($(2L/\lambda)_{res}$ for $B_{in} = 0$ and $(kL)_{res}$ for $|S_{11}| = |S_{11}|_{min}$) are defined rather precisely, and the calculated curves for the normalized current amplitudes ($|J(s)|/|J|_{max}$) agree with the experimental data within acceptable limits. Thus, the formulas for the current obtained by a first approximation of the averaging method are applicable to the calculation of vibrator integral characteristics

such as the radiated (scattered) electromagnetic field in all field zones, and to the investigation of the resonant properties of the vibrator.

As was indicated in Sect. 1.5, the solution of (2.7) can be obtained by an improved first approximation. This means that the transition from (2.7) to (2.8) is accomplished by the substitution $-(d\bar{A}(s)/ds) \sin ks + (d\bar{B}(s)/ds) \cos ks = \alpha i \omega E_{0s}(s)$. Then the input impedance of the vibrator is

$$Z_{in}^{imp} = \left(\frac{60i\tilde{k}}{\alpha k} \right) \frac{\cos \tilde{k}L + \alpha P_L^s(kr, \tilde{k}L)}{\sin \tilde{k}L + \alpha P_{\delta L}(kr, \tilde{k}L) + [\sin \tilde{k}L + \alpha P_{\delta 1}(kr, \tilde{k}L) + \alpha^2 P_{\delta 2}(kr, \tilde{k}L)]}. \quad (2.27)$$

Here

$$\begin{aligned} P_{\delta 1}(kr, \tilde{k}L) &= P_{\delta L}(kr, \tilde{k}L) + \sin \tilde{k}L P_0^s(kr, \tilde{k}L) - \cos \tilde{k}L P_{\delta 0}(kr, \tilde{k}L), \\ P_{\delta 2}(kr, \tilde{k}L) &= P_{\delta L}(kr, \tilde{k}L) P_0^s(kr, \tilde{k}L) - P_L^s(kr, \tilde{k}L) P_{\delta 0}(kr, \tilde{k}L), \\ P_0^s(kr, \tilde{k}L) &= \int_{-L}^L \frac{e^{-ikR(s,0)}}{R(s,0)} \cos \tilde{k}s \, ds, \quad P_{\delta 0}(kr, \tilde{k}L) = \int_{-L}^L \frac{e^{-ikR(s,0)}}{R(s,0)} \sin \tilde{k}|s| \, ds. \end{aligned} \quad (2.28)$$

The curves calculated by (2.27) are given in Figs. 2.6 and 2.7 as dotted lines, well correlated with the solution (2.26). The cumbersome formulas derived by solving (2.7) by the averaging method to second approximation improve the accuracy of the results but are useless in practice. However, the accuracy of a mathematical model may be enhanced by other methods, as will be demonstrated below.

2.2.1 Impedance Vibrator with Lumped Load in the Center

The problem of impedance vibrator excitation by an EMF δ -generator can be used for analysis of passive vibrators with lumped load. The current in a symmetric vibrator loaded by lumped impedance Z_{cL} at $s = 0$ and located in the field of a plane electromagnetic wave is defined by a combination of two current distributions ([11] in Chap. 1):

$$J_r(s) = J_{sc}(s) - J_{tr}(s), \quad (2.29)$$

where $J_{sc}(s)$ is the current in the gapless vibrator and $J_{tr}(s)$ is the current in the vibrator excited by the δ -generator. The current $J_{sc}(s)$ in the gapless scattering vibrator with accuracy to the terms of order α^2 is given, according to (2.13), by

$$\begin{aligned}
J_{sc}(s) = & -\alpha E_0 \cos \psi \sin \theta \frac{i\omega/(k\tilde{k})}{1 - (q/\tilde{k})^2} \\
& \times \left[\frac{\cos \tilde{k}s \cos qL - \cos \tilde{k}L \cos qs}{\cos \tilde{k}L + \alpha P_L^s(kr, \tilde{k}L)} + i \frac{\sin \tilde{k}s \sin qL - \sin \tilde{k}L \sin qs}{\sin \tilde{k}L + \alpha P_L^a(kr, \tilde{k}L)} \right],
\end{aligned} \tag{2.30}$$

where $E_{0s}(s) = E_0 \cos \psi \sin \theta e^{iks \cos \theta}$. Here $q = k \cos \theta$, E_0 is the incident wave amplitude, ψ is the angle between the vibrator axis and the polarization plane of the incident wave, the angle θ is measured from the vibrator axis, and

$$\begin{aligned}
P_L^a(kr, \tilde{k}L) = & - \int_{-L}^L G(s, L) \sin \tilde{k}s ds \\
= & \sin \tilde{k}L \left\{ 2 \ln 2 - \gamma(L) - \frac{1}{2} [\text{Cin}(2\tilde{k}L + 2kL) + \text{Cin}(2\tilde{k}L - 2kL)] \right. \\
& \left. - \frac{i}{2} [\text{Si}(2\tilde{k}L + 2kL) - \text{Si}(2\tilde{k}L - 2kL)] \right\} \\
& - \cos \tilde{k}L \left\{ \frac{1}{2} [\text{Si}(2\tilde{k}L + 2kL) + \text{Si}(2\tilde{k}L - 2kL)] \right. \\
& \left. - \frac{i}{2} [\text{Cin}(2\tilde{k}L + 2kL) - \text{Cin}(2\tilde{k}L - 2kL)] \right\}.
\end{aligned} \tag{2.31}$$

The current $J_{tr}(s)$ is calculated by (2.16) if V_0 is replaced by V_{cL} ,

$$V_{cL} = J_{sc}(0) \frac{Z_{in} Z_{cL}}{Z_{in} + Z_{cL}}. \tag{2.32}$$

Then the current in the load of the receiving antenna has the form

$$\begin{aligned}
J_r(0) = & J_{sc}(0) \frac{Z_{in}}{Z_{in} + Z_{cL}} = \alpha E_0 \cos \psi \sin \theta \frac{i\omega/(k\tilde{k})}{1 - (q/\tilde{k})^2} \\
& \times \left[\frac{(\cos \tilde{k}L - \cos qL) + \alpha P_L^s(kr, \tilde{k}L)}{\cos \tilde{k}L + \alpha P_L^s(kr, \tilde{k}L)} \right] \frac{Z_{in}}{Z_{in} + Z_{cL}}.
\end{aligned} \tag{2.33}$$

2.2.2 Surface Impedance of Thin Vibrators

As discussed above, in comparative numerical calculations for perfectly conducting vibrators the value of the distributed surface impedance \bar{Z}_S is set equal to zero.

However, the analysis of certain vibrators requires formulas for the numerical estimation of the surface impedance. Let us consider the problem of axisymmetric excitation of an infinite double-layer cylinder with outer radius r and inner radius r_i by a converging cylindrical wave. Let us introduce the cylindrical coordinate system ρ, φ, z with z -axis directed along the cylinder's axis. By symmetry, the electromagnetic field has only E_z and H_φ components, depending only on ρ . The medium has permittivity ε and permeability μ in the region $r - r_i$, and ε_i, μ_i when $\rho \leq r_i$.

The surface impedance $\bar{Z}_S = E_z/H_\varphi$ at $\rho = r$ may be found as a solution of Maxwell's equations expressed in terms of Bessel function $I_{0,1}$ and Neumann function $N_{0,1}$ as

$$\begin{aligned} \begin{Bmatrix} iE_z \\ H_\varphi \end{Bmatrix} &= \begin{Bmatrix} I_0(k\sqrt{\varepsilon\mu}r) + N_0(k\sqrt{\varepsilon\mu}r) \\ I_1(k\sqrt{\varepsilon\mu}r) + N_1(k\sqrt{\varepsilon\mu}r) \end{Bmatrix} \\ &\times \sqrt{\frac{\mu}{\varepsilon}} \frac{\sqrt{\frac{\varepsilon}{\mu}} N_1(k\sqrt{\varepsilon\mu}r_i) I_0(k\sqrt{\varepsilon_i\mu_i}r_i) - \sqrt{\frac{\varepsilon_i}{\mu_i}} N_0(k\sqrt{\varepsilon\mu}r_i) I_1(k\sqrt{\varepsilon_i\mu_i}r_i)}{\sqrt{\frac{\varepsilon_i}{\mu_i}} I_0(k\sqrt{\varepsilon\mu}r_i) I_1(k\sqrt{\varepsilon_i\mu_i}r_i) - \sqrt{\frac{\varepsilon}{\mu}} I_1(k\sqrt{\varepsilon\mu}r_i) I_0(k\sqrt{\varepsilon_i\mu_i}r_i)}. \end{aligned} \quad (2.34)$$

Assuming $r_i = 0$ and $|\varepsilon| \gg 1$ ($\varepsilon = \varepsilon' + 4\pi\sigma/i\omega$), we obtain the familiar formula for the impedance of a cylindrical conductor [3, 4], with the skin effect

$$\bar{Z}_S = \frac{k'}{120\pi\sigma} \frac{I_0(k'r)}{I_1(k'r)}, \quad (2.35)$$

where $k' = (1 - i)/\Delta^0$, $\Delta^0 = \omega/k\sqrt{2\pi\sigma\omega\mu}$ is the skin-layer thickness, and σ is the conductivity of the metal.

Consider corrugated ($L_1 \approx L_2$) or ribbed ($L_1 \ll L_2$) conductors (here L_1 is the ridge thickness, where $\bar{Z}_S = 0$, and L_2 is the cavity width, where $\bar{Z}_S \neq 0$) with cell periods $(L_1 + L_2) \ll \lambda/\sqrt{\varepsilon\mu}$ and $|\varepsilon_i| \gg 1$. Averaging the impedances over the cell period and taking into account (2.34), we have

$$\bar{Z}_S = -i \frac{L_2}{L_1 + L_2} \sqrt{\frac{\mu}{\varepsilon}} \frac{I_0(k\sqrt{\varepsilon\mu}r) N_0(k\sqrt{\varepsilon\mu}r_i) - I_0(k\sqrt{\varepsilon\mu}r_i) N_0(k\sqrt{\varepsilon\mu}r)}{I_1(k\sqrt{\varepsilon\mu}r) N_0(k\sqrt{\varepsilon\mu}r_i) - I_0(k\sqrt{\varepsilon\mu}r_i) N_1(k\sqrt{\varepsilon\mu}r)}, \quad (2.36)$$

which is valid for conductors with an isolating covering made of a magneto-dielectric [2] ($L_1 = 0$), and also for metallic cylinders ($r_i = 0$) with transverse dielectric insertions ($L_2 \ll L_1$).

For thin vibrators ($|(k\sqrt{\varepsilon\mu}r)^2 \ln(k\sqrt{\varepsilon\mu}r_i)| \ll 1$), the surface impedance does not depend on the excitation mode, and the corresponding boundary conditions become impressed [8], that is, they do not depend upon the structure of exciting field. Then with (2.34)–(2.36) we find that the complex impedances $\bar{Z}_S = \bar{R}_S + i\bar{X}_S$ for vibrators in thin-wire approximation equal

$$\bar{Z}_S = \frac{1 + i}{120\pi\sigma\Delta^0} \quad (2.37)$$

for a solid metallic cylinder if $r \gg \Delta^0$; note that $\bar{Z}_S = 0$ for a perfect conductor ($\sigma \rightarrow \infty$);

$$\bar{Z}_S = \frac{1}{120\pi\sigma h_0 + ikr(\varepsilon - 1)/2} \quad (2.38)$$

for a dielectric cylinder with thin metal covering ($h_0 \ll \Delta^0, \varepsilon = 1$);

$$\bar{Z}_S = \frac{1}{120\pi\sigma h_0} \quad (2.39)$$

for a metallic tubular cylinder $r \ll \Delta^0$ (“nanoradius” vibrator [4] $h_0 = r, r \ll \Delta^0$); and after substitution $h_0 = 0$ in (2.38),

$$\bar{Z}_S = -i \frac{2}{kr(\varepsilon - 1)} \quad (2.40)$$

for a dielectric cylinder;

$$\bar{Z}_S = -i \frac{L_2}{L_1 + L_2} \frac{2}{kr\varepsilon} \quad (2.41)$$

for a metal-dielectric cylinder;

$$\bar{Z}_S = \frac{1}{120\pi\sigma h_0 - i/kr\mu \ln(r/r_i)} \quad (2.42)$$

for a magnetodielectric metalized cylinder with inner conducting cylinder $r = r_i$ (2.39); and if $h_0 = 0$, then

$$\bar{Z}_S = ikr\mu \ln \frac{r}{r_i} \quad (2.43)$$

for a metallic cylinder with magnetodielectric covering (thickness $r - r_i$ [2]) or a ribbed cylinder;

$$\bar{Z}_S = \frac{i}{2} kr \cot^2 \psi \quad (2.44)$$

for a metallic monofilar helix with radius r ($kr \ll 1$) and winding angle ψ .

Formulas (2.37)–(2.44) have been obtained in the framework of impedance conception ([3] in Chap. 1, [8]), and they are valid for thin cylinders both with finite and infinite extension located in free space. If the vibrator is situated in a material

medium with parameters ε_1 and μ_1 , then all formulas must be multiplied by $\sqrt{\mu_1/\varepsilon_1}$. Since the surface impedance often depends on the parameters ε and μ , it is possible to alter the characteristics of antennas with fixed geometric dimensions by varying these parameters if they depend on the external static electrical and/or magnetic fields. It also follows from (2.43) and (2.44) that it is possible for vibrators with pure inductive surface impedance to define a term known as effective vibrator length $2L_{\text{eff}}$ [9]:

$$2L_{\text{eff}} = \left[1 + \frac{\mu \ln(r/r_i)}{2 \ln(2L/r)} \right] 2L, \quad 2L_{\text{eff}} = \left[1 + \frac{\cot^2 \psi}{4 \ln(2L/r)} \right] 2L, \quad (2.45)$$

that is, the impedance vibrator length $2L$ is “equivalent” to the perfectly conducting vibrator with the length $2L_{\text{eff}}$ with $2L_{\text{eff}} > 2L$.

2.2.3 Resonant Properties of Impedance Vibrators in Free Space

Near the resonance, when $\tilde{k}L \approx \pi/2$ and $\sin \tilde{k}L \approx 1$, it is possible to neglect the second summand in the denominator of (2.33), proportional to the small parameter α . If vibrator impedance is purely reactive, i.e., $\bar{R}_s = 0$, then defining the resonant condition as $X_{\text{in}} = 0$, we obtain the transcendental equation, allowing us to find the length (frequency) of the resonant vibrator,

$$\cos(\tilde{k}L)_{\text{res}} + \alpha \operatorname{Re} P_L^s(kr, (\tilde{k}L)_{\text{res}}) = 0, \quad (2.46)$$

where $\operatorname{Re} P_L^s$ is the real part of P_L^s , defined by (2.17). Let us remark that, as it will be shown below, the real part of the impedance vibrator has no considerable influence on its resonant properties.

Let us obtain an approximate solution of (2.46), expanding the unknown value $(\tilde{k}L)_{\text{res}}$ in a power series in the small parameter α :

$$(\tilde{k}L)_{\text{res}} = (\tilde{k}L)_0 + \alpha(\tilde{k}L)_1 + \alpha^2(\tilde{k}L)_2 + \dots \quad (2.47)$$

Substituting (2.47) into (2.46) and equating summands with equal powers, we have

$$(\tilde{k}L)_{\text{res}} \approx \frac{\pi}{2} + \alpha \operatorname{Re} P_L^s\left(\frac{\pi r}{2L}, \frac{\pi}{2}\right), \quad (2.48)$$

with accuracy to terms of order α^2 . With (2.17), (2.48) may be transformed into

$$(\tilde{k}L)_{\text{res}} \approx \frac{\pi}{2} + \alpha \left[\frac{1}{2} \operatorname{Si}(2\pi - 2\chi L) + \frac{1}{2} \operatorname{Si}(2\chi L) \right], \quad (2.49)$$

where $\chi = -\alpha(\bar{X}_S/r)$. Assuming $(2L)_{\text{res}} \approx \lambda/2$ and taking into consideration that $\alpha = 1/(2 \ln(2r/\lambda))$, $2\chi L = -\alpha(\lambda\bar{X}_S/2r)$, $\tilde{k} = k(1 - \alpha(\bar{X}_S/kr))$, we obtain the formula for the vibrator resonant length as a function of its radius r , wavelength λ , and surface impedance \bar{X}_S :

$$(2L)_{\text{res}} \approx \frac{\lambda}{2} \frac{1}{1 - \alpha \frac{\bar{X}_S}{kr}} + \alpha \frac{1}{k \left(1 - \alpha \frac{\bar{X}_S}{kr}\right)} \left[\text{Si} \left(2\pi + \alpha \frac{\lambda\bar{X}_S}{2r} \right) - \text{Si} \left(\alpha \frac{\lambda\bar{X}_S}{2r} \right) \right]. \quad (2.50)$$

Expression (2.50) may be simplified for relatively small values of the normalized surface impedance ($\bar{X}_S \sim kr$) and represented as

$$(2L)_{\text{res}} \approx \frac{\lambda}{2} - \frac{\lambda}{4\pi \ln \frac{\lambda}{2r}} \left(\text{Si}(2\pi) + \frac{\lambda\bar{X}_S}{2r} \right). \quad (2.51)$$

We note that (2.51) was derived by the power series expansion

$$\frac{1}{1 - \alpha \left(\frac{\bar{X}_S}{kr} \right)} = 1 + \alpha \left(\frac{\bar{X}_S}{kr} \right) - \alpha^2 \left(\frac{\bar{X}_S}{kr} \right)^2 + \dots \approx 1 + \alpha \left(\frac{\bar{X}_S}{kr} \right).$$

It was shown in Sect. 2.2.2 that if $\bar{X}_S > 0$ (the inductive impedance has, for example, a metallic conductor covered by a magnetodielectric layer, a corrugated cylindrical conductor, or a monofilar metallic helix), then the surface impedance of a thin vibrator can be represented as $\bar{X}_S = krC_L$; and if $\bar{X}_S < 0$ (capacitive impedance has, for example, a dielectric or a layered metal-dielectric cylinder), then $\bar{X}_S = -kr[C_C/(kr)^2]$, where the constants C_L and C_C are defined by the geometric dimension and electrophysical parameters of the vibrator material. Bearing this in mind, we transform (2.51) into

$$(2L)_{\text{res}} \approx \frac{\lambda}{2} - \frac{\lambda}{4 \ln \frac{\lambda}{2r}} \left(\frac{\text{Si}(2\pi)}{\pi} + \frac{\bar{X}_S}{kr} \right). \quad (2.52)$$

As follows from (2.52), the resonant length of a thin vibrator in free space can be either shorter or longer than $\lambda/2$ (vibrator shortening or lengthening, respectively), depending on the distributed surface impedance type. Note the principal difference for perfect conductivity ($\bar{X}_S = 0$), where $(2L)_{\text{res}} < (\lambda/2)$ for any finite r/λ . This is illustrated in Fig. 2.10a, where the normalized resonant length in dependence on the vibrator radius for capacitive and inductive impedances, and also for a perfectly conducting vibrator, is shown. For comparison, results obtained by the iterations method to a second approximation in [12] in Chap. 1 (the formula (2.26)) are presented. For the capacitive impedance (curves 1 and 2), lengthening $(2L)_{\text{res}}$

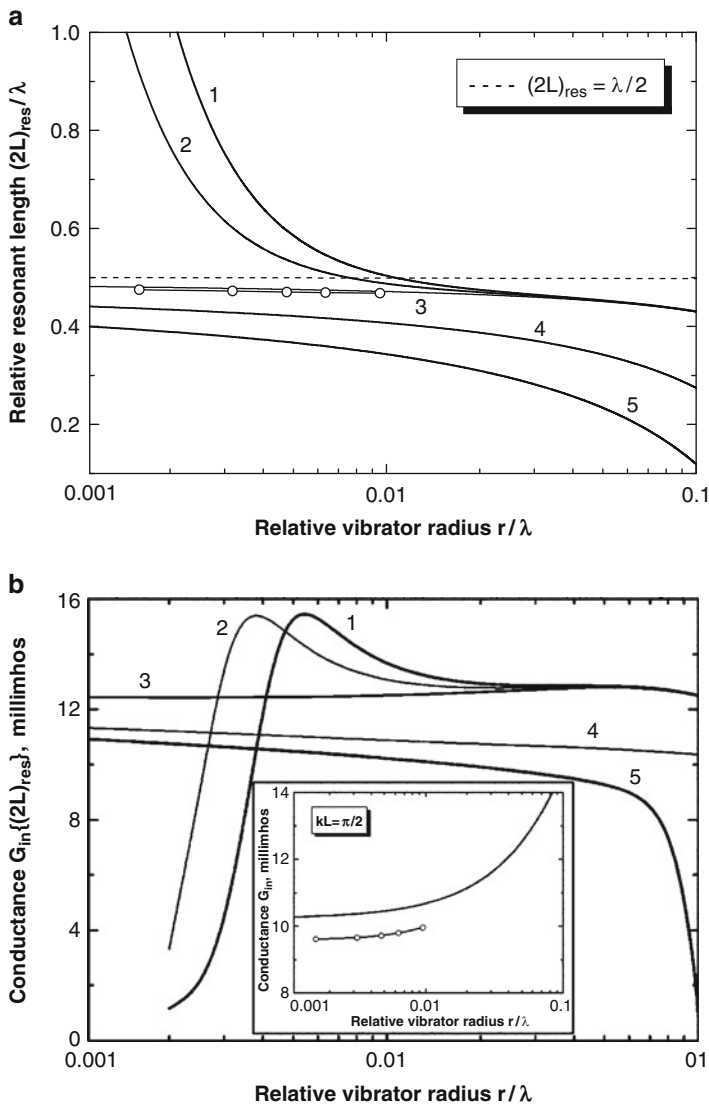


Fig. 2.10 The relative resonant length and the input conductance versus vibrator radius: 1 $\bar{Z}_S = -i\bar{X}_S(C_C = 0.002)$; 2 $\bar{Z}_S = -i\bar{X}_S(C_C = 0.001)$; 3 $\bar{Z}_S = 0$ (the circles correspond to calculation [12] in Chap. 1); 4 $\bar{Z}_S = i\bar{X}_S(C_L = 1.0)$; 5 $\bar{Z}_S = i\bar{X}_S(C_L = 2.0)$

transits to shortening as the radius increases, reaching for some r/λ the value $(2L)_{\text{res}} = \lambda/2$ (a half-wave vibrator). For a perfectly conducting vibrator (curve 3 and the circles) and for inductive impedance (curves 4 and 5), the resonant tuning

requires that vibrator length be decreased as compared to that of a half-wave vibrator, and such shortening grows with an increase in the distributed surface impedance.

It is interesting to observe how the radius of the resonant impedance vibrator influences the real part of the input admittance (Fig. 2.10b). The input conductance $G_{\text{in}}\{(2L)_{\text{res}}\}$ increases monotonically with increase in the radius (small windows in Fig. 2.10b) for the half-wave ($kL = \pi/2$, $2L = \lambda/2$) perfectly conducting vibrator, but it remains practically constant (curve 3) for the resonant vibrator. The distributed surface impedance influences in an essential way the radial dependence of the real part of input admittance of the vibrator.

2.3 Impedance Vibrators in an Infinite Homogeneous Lossy Medium

In some important practical applications such as underground and underwater radio communication, geophysical investigations, medical diagnostics and hyperthermia, a vibrator antenna must work in a medium with electrophysical parameters that differ significantly from those of air. Theoretical and experimental works concerning antennas in different medium are covered, systemized, and generalized in the monograph [10], where original results for “nonisolated” and “isolated” vibrator antennas in a lossy medium are presented. The terms “isolated” and “nonisolated” are related to antennas with or without a multilayered dielectric shell, respectively. The integral equations for the current in these two cases coincide formally, but their kernels differ essentially. Therefore, the solution of the integral equations for “nonisolated” and the “isolated” antennas requires separate considerations, and moreover, the choice of solution method depends on environmental parameters. Approximate expressions for the vibrator current, obtained in [10], are valid for electrical length $(2L/\lambda_1) \leq 1.25$, where λ_1 is the wavelength in the medium. It was also noted in [10, 11] that the rate of field amplitude decrease when the distance from the dipole increases in a material medium is essentially greater than in free space, and moreover, it is substantially different for the near, intermediate, and far antenna zones. At the same time, the characteristics of real vibrators with finite dimensions comparable with the wavelength in the material medium differ essentially from the corresponding parameters of electrically short dipoles. Hence, taking into account possible fields of application of vibrator antennas located in different medium a thorough analysis of the spatial field distribution in a near-field zone of the vibrator (especially when it has complex distributed impedance) is of real practical interest.

In this section we will consider thin impedance vibrators located in an infinite homogeneous medium with sufficiently arbitrary parameters, including those for a conducting medium without any restrictions on vibrator lengths and excitation methods.

The analysis is based on the integrodifferential equation

$$\left(\frac{d^2}{ds^2} + k_1^2\right) \int_{-L}^L J(s') \frac{e^{-ik_1 R(s,s')}}{R(s,s')} ds' = -i\omega\varepsilon_1 E_{0s}(s) + i\omega\varepsilon_1 z_i J(s), \quad (2.53)$$

where $k_1 = k\sqrt{\varepsilon_1\mu_1} = k'_1 - ik''_1$ is the wave number in the medium and $\varepsilon_1 \neq 1$, $\mu_1 \neq 1$, $z_i(s) = \text{const}$. We obtain the solution of (2.53) as we did that of (2.1), i.e., by the change of variables

$$\begin{aligned} J(s) &= A(s) \cos k_1 s + B(s) \sin k_1 s, \\ \frac{dJ(s)}{ds} &= -A(s)k_1 \sin k_1 s + B(s)k_1 \cos k_1 s. \end{aligned} \quad (2.54)$$

Using the methods described in Sect. 2.1, we obtain an approximate expression for the current in a thin impedance vibrator located in an infinite homogeneous lossy medium:

$$\begin{aligned} J(s) &= \alpha \frac{i\omega\varepsilon_1}{k_1} \left\{ \int_{-L}^s E_{0s}(s') \sin \tilde{k}_1(s-s') ds' \right. \\ &\quad - \frac{\sin \tilde{k}_1(L+s) + \alpha P^s[k_1 r, \tilde{k}_1(L+s)]}{\sin 2\tilde{k}_1 L + \alpha P^s(k_1 r, 2\tilde{k}_1 L)} \int_{-L}^L E_{0s}^s(s') \sin \tilde{k}_1(L-s') ds' \\ &\quad \left. - \frac{\sin \tilde{k}_1(L+s) + \alpha P^a[k_1 r, \tilde{k}_1(L+s)]}{\sin 2\tilde{k}_1 L + \alpha P^a(k_1 r, 2\tilde{k}_1 L)} \int_{-L}^L E_{0s}^a(s') \sin \tilde{k}_1(L-s') ds' \right\}. \end{aligned} \quad (2.55)$$

Here $\tilde{k}_1 = k_1 + i(\alpha/r)\bar{Z}_S \sqrt{\varepsilon_1/\mu_1}$, $G(s, s') = \frac{e^{-ik_1 \sqrt{(s-s')^2 + r^2}}}{\sqrt{(s-s')^2 + r^2}}$,

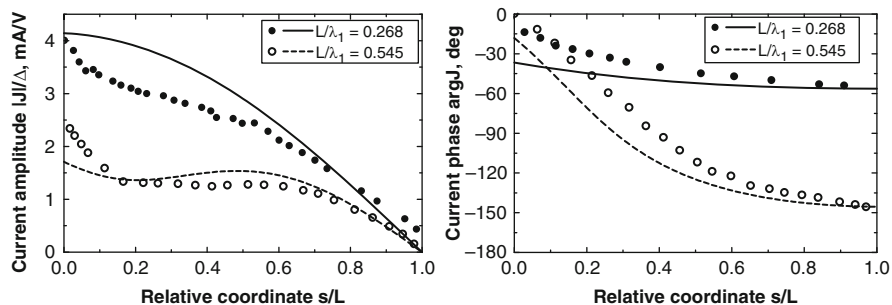
$$\begin{aligned} P^s[k_1 r, \tilde{k}_1(L+s)] &= \int_{-L}^s [G(s', -L) + G(s', L)] \sin \tilde{k}_1(s-s') ds' \Big|_{s=L} \\ &= P^s(k_1 r, 2\tilde{k}_1 L), \\ P^a[k_1 r, \tilde{k}_1(L+s)] &= \int_{-L}^s [G(s', -L) - G(s', L)] \sin \tilde{k}_1(s-s') ds' \Big|_{s=L} \\ &= P^a(k_1 r, 2\tilde{k}_1 L). \end{aligned} \quad (2.56)$$

If the vibrator is excited by a lumped EMF at the center, the expression for the current (2.55) has the form

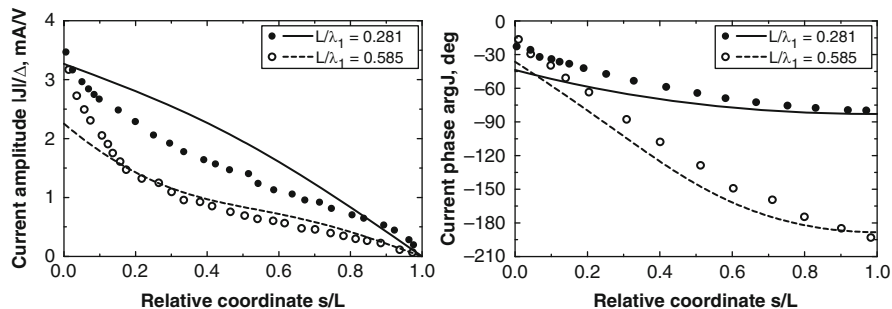
$$J(s) = -\alpha V_0 \left(\frac{i\omega\varepsilon_1}{2\tilde{k}_1} \right) \frac{\sin \tilde{k}_1(L-|s|) + \alpha P_\delta^s(k_1 r, \tilde{k}_1 s)}{\cos \tilde{k}_1 L + \alpha P_L^s(k_1 r, \tilde{k}_1 L)}. \quad (2.57)$$

Here the equality $P_{\delta}^s(k_1 r, \tilde{k}_1 s) = P^s[k_1 r, \tilde{k}_1 (L + s)] - (\sin \tilde{k}_1 s + \sin \tilde{k}_1 |s|) P_L^s(k_1 r, \tilde{k}_1 L)$, $P^s[k_1 r, \tilde{k}_1 (L + s)]$ is defined by (2.56), and $P_L^s(k_1 r, \tilde{k}_1 L) = \int_{-L}^L G(s, L) \cos \tilde{k}_1 s ds$.

a



b



c

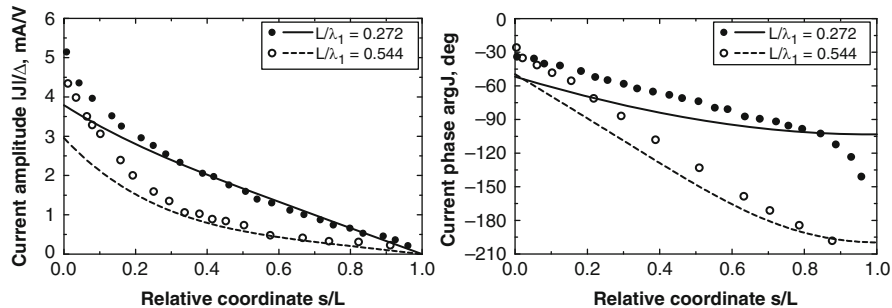


Fig. 2.11 The amplitude–phase distributions of the current for the vibrator in saltwater with different salt concentrations ($\Delta = \lambda/\lambda_1$). (a) $\varepsilon'_1 = 83.46$, $(\tan \delta)_1 = 0.662$, $k''_1/k'_1 = 0.301$, $f = 28$ MHz, $r/\lambda_1 = 0.0028$, $\Delta = 9.58$ (b) $\varepsilon'_1 = 102.14$, $(\tan \delta)_1 = 1.823$, $k''_1/k'_1 = 0.592$, $f = 28$ MHz, $r/\lambda_1 = 0.0037$, $\Delta = 12.54$ (c) $\varepsilon'_1 = 139.3$, $(\tan \delta)_1 = 32.83$, $k''_1/k'_1 = 0.97$, $f = 14$ MHz, $r/\lambda_1 = 0.0072$, $\Delta = 48.75$

To validate approximate analytical solution for the current (2.57), Fig. 2.11 shows the amplitude–phase distributions of the current for the perfectly conducting vibrator ($\bar{Z}_S = 0$), calculated and plotted for different vibrator lengths and medium absorption coefficients, together with the experimental values from [5] (the circles). Since theoretical and experimental curves agree well, we may conclude that the proposed mathematical model corresponds to the real electromagnetic process.

As we may suppose, the electrophysical parameters of the environment influence sufficiently the amplitude–phase distributions of the current in the vibrator. This can be proved by the plots in Fig. 2.12, where are shown curves for the normalized amplitude $|J(s)|/|J|_{\max}$ and the current phase $\arg J(s)$ along the arm of a symmetric perfectly conducting half-wave vibrator located in a biological medium with the electrophysical parameters given in Table 2.1.

Figure 2.12 demonstrates the variation in the electrical length of a vibrator $2L/\lambda_1$ in a material medium, proved by additional extrema and the sections with opposite phases in the distributions of the current along the vibrator, and this variation increases with the density of the medium.

2.4 Radiation Fields of Impedance Vibrators in Infinite Medium

Expressions (2.57), (1.3), and (1.12) define the radiation fields of a thin impedance vibrator in a material medium. These fields may be written in spherical coordinates ρ, θ, φ (θ is the angle measured from the vibrator axis) as

$$\begin{aligned}
 E_\rho(\rho, \theta) &= \frac{k_1}{\omega \varepsilon_1} \int_{-L}^L J(s) \frac{e^{-ik_1 R(s)}}{R^3(s)} \left\{ 2R(s) \left[1 + \frac{1}{ik_1 R(s)} \right] \cos \theta \right. \\
 &\quad \left. - ik_1 \rho \left[1 + \frac{3}{ik_1 R(s)} - \frac{3}{k_1^2 R^2(s)} \right] s \sin^2 \theta \right\} ds, \\
 E_\theta(\rho, \theta) &= -\frac{k_1 \sin \theta}{\omega \varepsilon_1} \int_{-L}^L J(s) \frac{e^{-ik_1 R(s)}}{R^3(s)} \left\{ 2R(s) \left[1 + \frac{1}{ik_1 R(s)} \right] \right. \\
 &\quad \left. - ik_1 \rho \left[1 + \frac{3}{ik_1 R(s)} - \frac{3}{k_1^2 R^2(s)} \right] (\rho - s \cos \theta) \right\} ds, \\
 H_\varphi(\rho, \theta) &= \frac{ik_1 k \sin \theta}{\omega} \int_{-L}^L J(s) \frac{e^{-ik_1 R(s)}}{R^2(s)} \left[1 + \frac{1}{ik_1 R(s)} \right] \rho ds, \\
 E_\varphi(\rho, \theta) &= H_\rho(\rho, \theta) = H_\theta(\rho, \theta) = 0, \quad R(s) = \sqrt{\rho^2 - 2\rho s \cos \theta + s^2},
 \end{aligned} \tag{2.58}$$

and the power absorbed in a unit volume of dielectric is given by

$$\bar{P}(\rho, \theta) \sim |\vec{E}(\rho, \theta)|^2 \omega \varepsilon_1'', \tag{2.59}$$

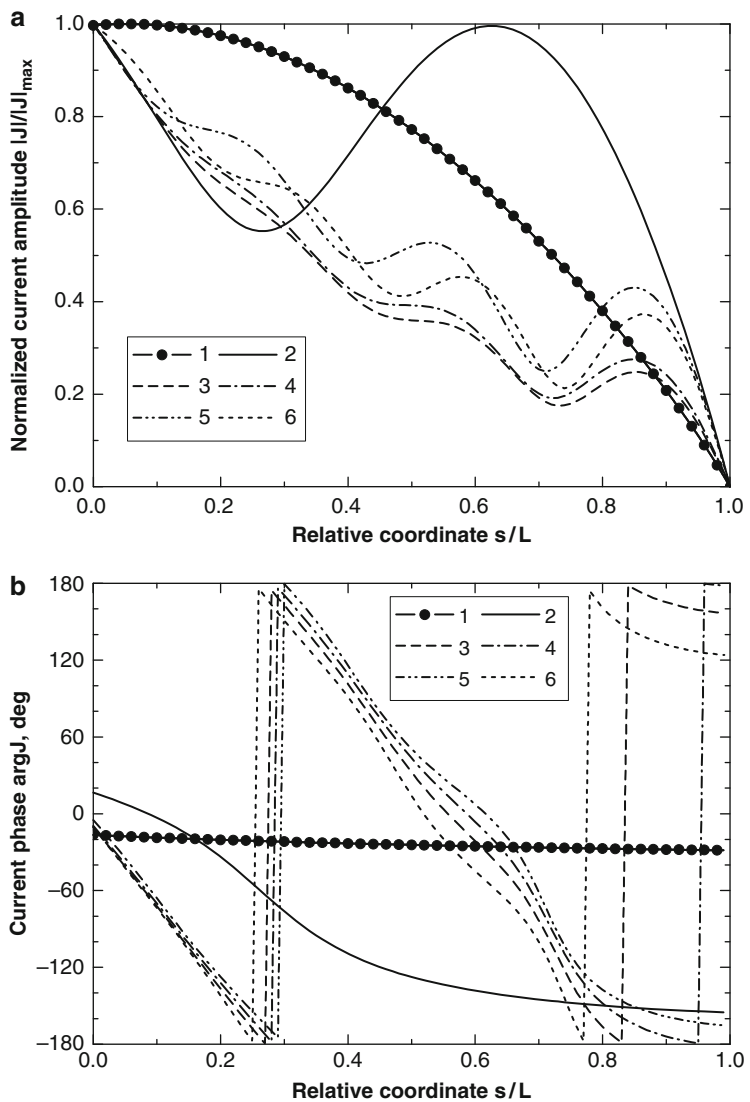


Fig. 2.12 The amplitude–phase distributions of the current for a perfectly conducting vibrator in different medium for $r/\lambda = 0.007022$ and $2L/\lambda = 0.5$: 1 free space; 2 fat layer; 3 muscular tissue; 4 skin; 5 liver; 6 whole blood

Table 2.1 The electrophysical parameters ($\varepsilon_1 = \varepsilon'_1 - i\varepsilon''_1$, $(\tan \delta)_1 = \varepsilon''_1/\varepsilon'_1$) for human body tissues (the wavelength is $\lambda = 10$ cm and the temperature is 37°C [12])

Medium	ε'_1	ε''_1	$(\tan \delta)_1$
Free space	1.0	0.0	0.0
Fat layer	6.5	1.6	0.246
Muscular tissue	46.5	18.0	0.387
Skin	43.5	16.5	0.379
Liver	42.5	12.2	0.287
Whole blood	53.0	15.0	0.283

where $\vec{E}(\rho, \theta) = \vec{e}_\rho E_\rho(\rho, \theta) + \vec{e}_\theta E_\theta(\rho, \theta)$, $\varepsilon_1'' = 4\pi\sigma_1/\omega$, σ_1 is the medium conductivity, and \vec{e}_ρ and \vec{e}_θ are unit vectors.

Expressions for the fields of an electrically short vibrator (dipole) in a homogeneous isotropic lossy medium for $|k_1 L| \ll 1$ may be derived from (2.58) with $J(s) = J_0$ and $R(s) \approx \rho$:

$$E_\rho(\rho, \theta) = -i2LJ_0 \frac{2k_1^2 \cos \theta e^{-ik_1 \rho}}{\omega \varepsilon_1 \rho} \left(\frac{1}{k_1^2 \rho^2} + \frac{i}{k_1 \rho} \right), \quad (2.60a)$$

$$E_\theta(\rho, \theta) = -i2LJ_0 \frac{k_1^2 \sin \theta e^{-ik_1 \rho}}{\omega \varepsilon_1 \rho} \left(\frac{1}{k_1^2 \rho^2} + \frac{i}{k_1 \rho} - 1 \right), \quad (2.60b)$$

$$H_\varphi(\rho, \theta) = -i2LJ_0 \frac{k_1 k \sin \theta e^{-ik_1 \rho}}{\omega \rho} \left(\frac{i}{k_1 \rho} - 1 \right). \quad (2.60c)$$

The structure of the electromagnetic field in the immediate vicinity of the vibrator is rather complex. However, for $\rho \rightarrow \infty$ and $\rho \gg 2L$ ($R(s) \cong \rho - s \cos \theta$) we may substitute in (2.58)

$$\frac{1}{R(s)} \cong \frac{1}{\rho}, \quad e^{-ik_1 R(s)} \cong e^{-ik_1 \rho} e^{ik_1 s \cos \theta}, \quad (2.61)$$

and for $|k_1 \rho| \rightarrow \infty$, the radiation field has the form

$$\begin{aligned} E_\theta(\rho, \theta) &= \frac{ik_1^2}{\omega \varepsilon_1} \sin \theta \frac{e^{-ik_1 \rho}}{\rho} \int_{-L}^L J(s) e^{ik_1 s \cos \theta} ds, \\ H_\varphi(\rho, \theta) &= \frac{ik_1 k}{\omega} \sin \theta \frac{e^{-ik_1 \rho}}{\rho} \int_{-L}^L J(s) e^{ik_1 s \cos \theta} ds, \end{aligned} \quad (2.62)$$

and the characteristic impedance of the medium becomes $E_\theta/H_\varphi = \sqrt{\mu_1/\varepsilon_1}$.

In Fig. 2.13 (here and below, $\lambda = 10$ cm, $r/\lambda = 0.0033$) are shown the normalized amplitudes $|\bar{E}_s|^2 = |E_s|^2/|E_s|_{\max}^2$ for the field parallel to the axis of a half-wave vibrator, $E_s(\rho, \theta) = E_\rho(\rho, \theta) \cos \theta - E_\theta(\rho, \theta) \sin \theta$, as a function of surface impedance for different environmental parameters. As may be seen, the resonant tuning ($\tilde{k}_1 L \cong \pi/2$) requires that the distributed impedance of the vibrator in the lossy material should transit from capacitive ($\bar{X}_S < 0$) to inductive ($\bar{X}_S > 0$) type and that resonance should occur for higher values \bar{X}_S when ε_1' and ε_1'' are increased.

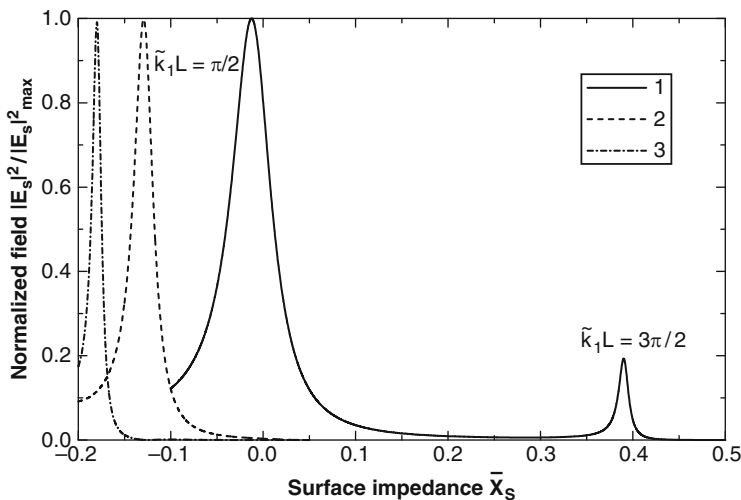


Fig. 2.13 Near-field amplitude versus the surface impedance of the vibrator for $kL = \pi/2$, $\rho/\lambda = 0.5$, $\theta = 90^\circ$: 1 free space; 2 fat layer; 3 muscular tissue

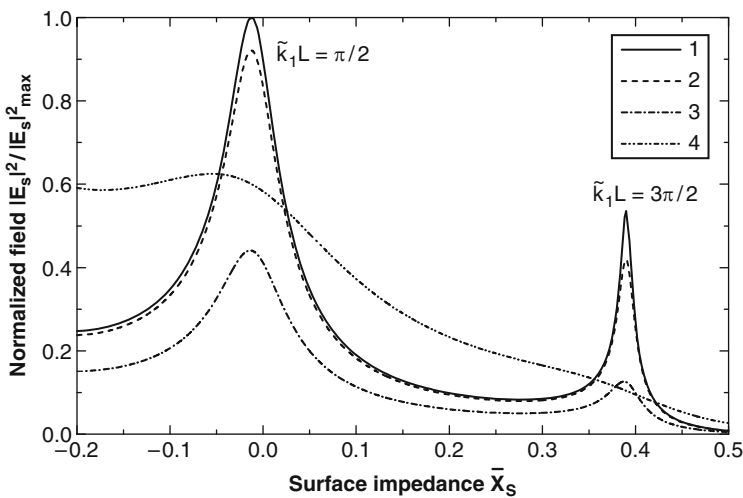


Fig. 2.14 The field amplitude in the far zone versus the surface impedance of the vibrator for $kL = \pi/2$, $\rho/\lambda = 10.0$, $\theta = 90^\circ$: 1 $\bar{R}_S = 0.0$; 2 $\bar{R}_S = 0.002$; 3 $\bar{R}_S = 0.01$; 4 $\bar{R}_S = 0.1$

Figure 2.14 represents the dependencies of the far-zone radiation field of a half-wave vibrator in free space upon \bar{X}_S for different real impedances \bar{R}_S . As expected, the field decreases in comparison to that of a perfectly conducting vibrator when \bar{R}_S is increased. Note that the vibrator could not be tuned for large values of \bar{R}_S ($\bar{R}_S \geq 0.1$).

The electrophysical parameters of the environment influence considerably the spatial distribution of the electromagnetic field radiated by the vibrator, and thus the absorbed power in the unit volume. This conclusion can be reached by analyzing the plots in Figs. 2.15–2.17, where the distributions of the radiation field for a half-wave impedance vibrator at different distances from its axis are presented for the resonant $\tilde{k}_1 L$ values in free space, the fat layer, and human muscular tissue at 37°C.

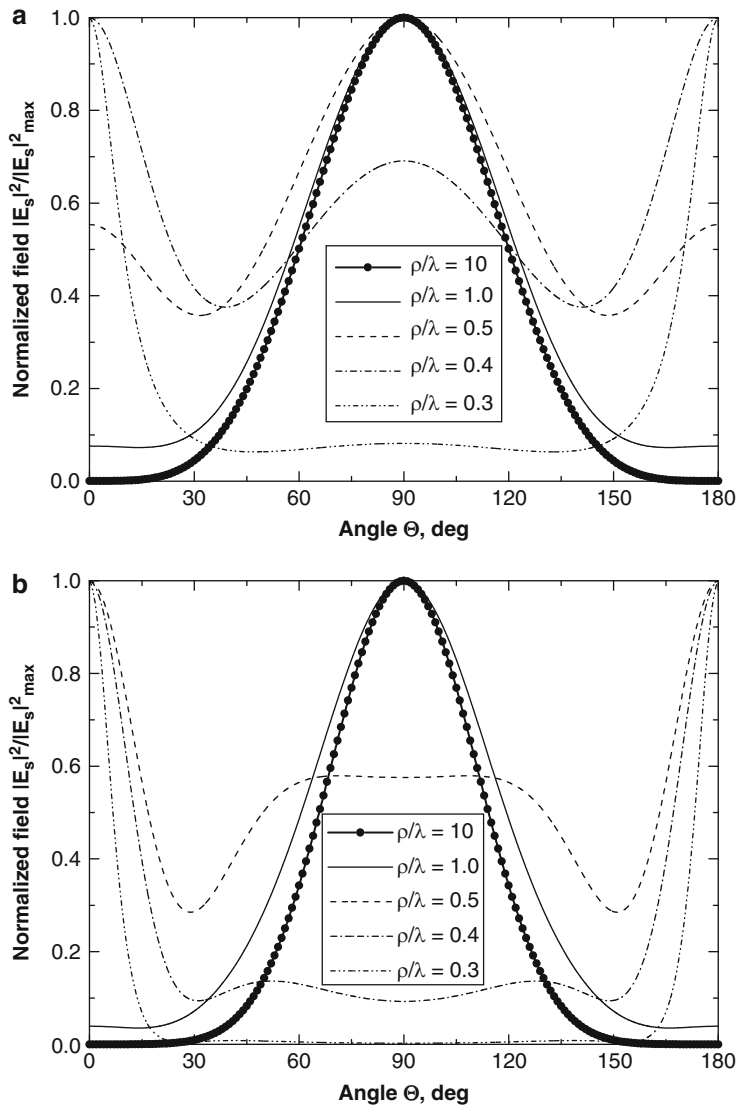


Fig. 2.15 The distribution of the radiation field of a vibrator in free space: (a) $\bar{X}_S = -0.013$ ($\tilde{k}_1 L = 0.47\pi$), (b) $\bar{X}_S = 0.39$ ($\tilde{k}_1 L = 1.44\pi$)

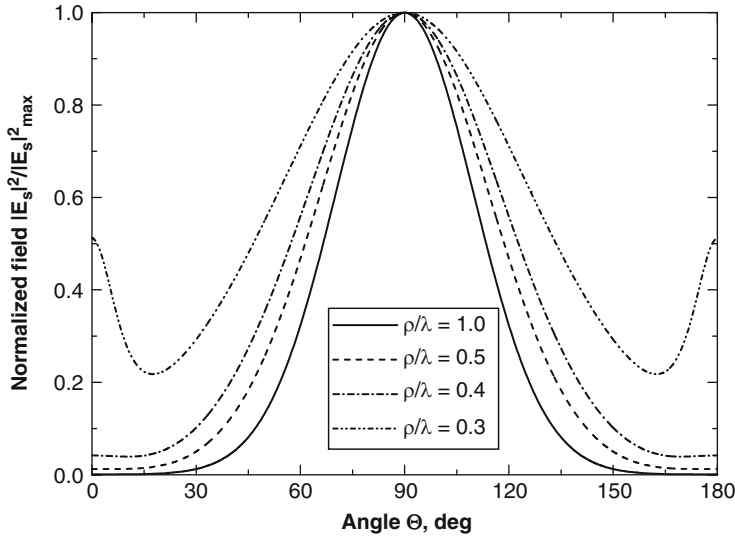


Fig. 2.16 The field distribution of the vibrator in the fat layer: $\bar{X}_S = -0.129(\tilde{k}_1 L = 0.47\pi)$

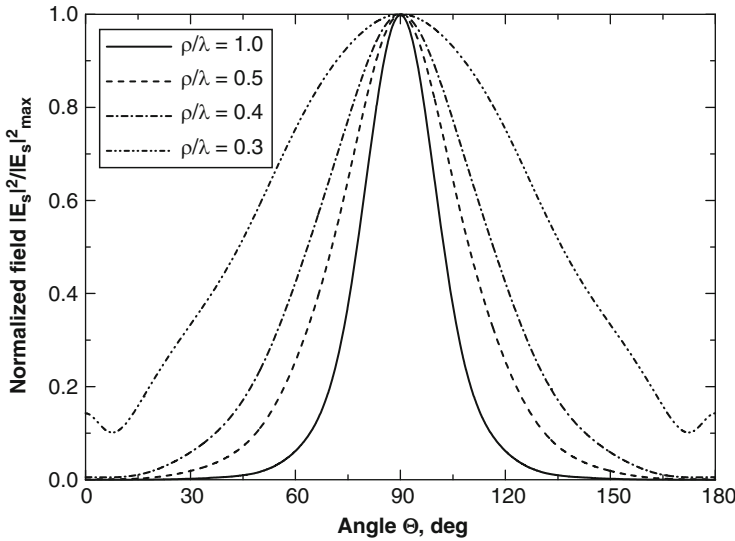


Fig. 2.17 The field distribution of the vibrator in muscular tissue: $\bar{X}_S = -0.18(\tilde{k}_1 L = 0.47\pi)$

The wire antennas are usually made of lossy materials, that is, the surface impedance is really complex, $\bar{Z}_S = \bar{R}_S + i\bar{X}_S$. The values \bar{Z}_S depend on the operating wavelength λ and the vibrator radius r , as shown in Sect. 2.2.2. Figure 2.18 demonstrates the dependence of the normalized field $|\bar{E}|^2$ for the vibrator radius

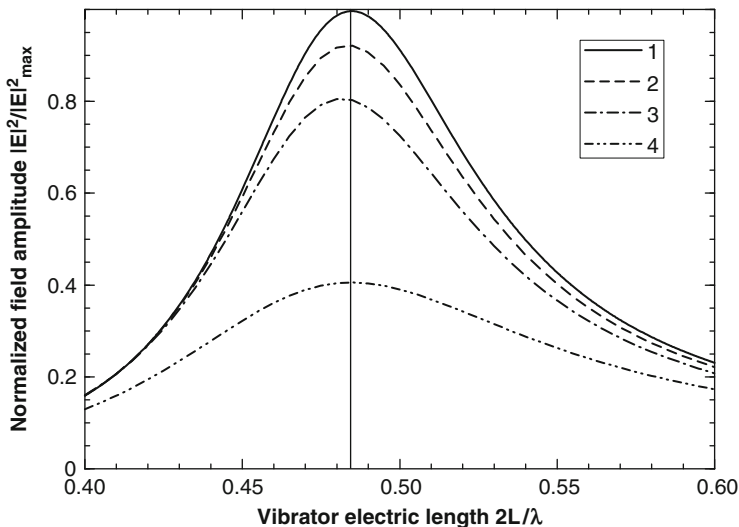


Fig. 2.18 The radiation field of the vibrator $|\bar{E}|^2$ versus electrical length $2L/\lambda$ for different materials for $\rho = \lambda$, $\theta = \pi/2$: 1 $z_i = 0$ [ohm/m] for a perfect conductor; 2 $z_i = 189 + i180$ [ohm/m] for copper; 3 $z_i = 527 + i458$ [ohm/m] for platinum; 4 $z_i = 2940 + i700$ [ohm/m] for bismuth. The impedance values are taken from [13]

$r = 0.00127$ cm at distance $\rho = \lambda$ along the vibrator normal ($\theta = \pi/2$) at wavelength $\lambda = 10$ cm upon the electrical length of vibrators made of different materials. As is evident from the graph, the vibrator material does not practically influence its resonant length, while the vibrator radiation efficiency decreases substantially as the active component of impedance \bar{R}_S increases.

This is also proved by the surface and contour plots in Fig. 2.19a, b, where the values, normalized by the maximal value of $|\bar{E}|^2$, for a half-wave vibrator versus the active \bar{R}_S and the reactive \bar{X}_S parts of its surface impedance are presented. Let us note that as \bar{R}_S increases, the bandwidth of the value \bar{X}_S where the vibrator is efficiently excited widens, reducing the requirements to the specification of \bar{R}_S and \bar{X}_S for an antenna with artificial complex impedance. In our calculations, the active part of the vibrator impedance was equated to $\bar{R}_S = 0.001$, since this value gives good coincidence between our formulas and real electrodynamic processes.

Since the resonant length of the vibrator essentially depends on the imaginary part of the impedance \bar{X}_S (Fig. 2.19c, d), a quarter-wave ($kL = \pi/4$, $2L = \lambda/4$) may be used instead of a half-wave vibrator by choosing \bar{X}_S for the material medium so that $\tilde{k}_1 L = \pi/2$ (Fig. 2.20), thus allowing antenna miniaturization for some applications. The spatial distribution of the normalized near fields for half-wave and quarter-wave vibrators in free space are shown in Fig. 2.21. As can be seen, the radiation field of the quarter-wave vibrator is more homogeneous than that of the half-wave vibrator at small distances. However, it decreases faster when the distance is increased.

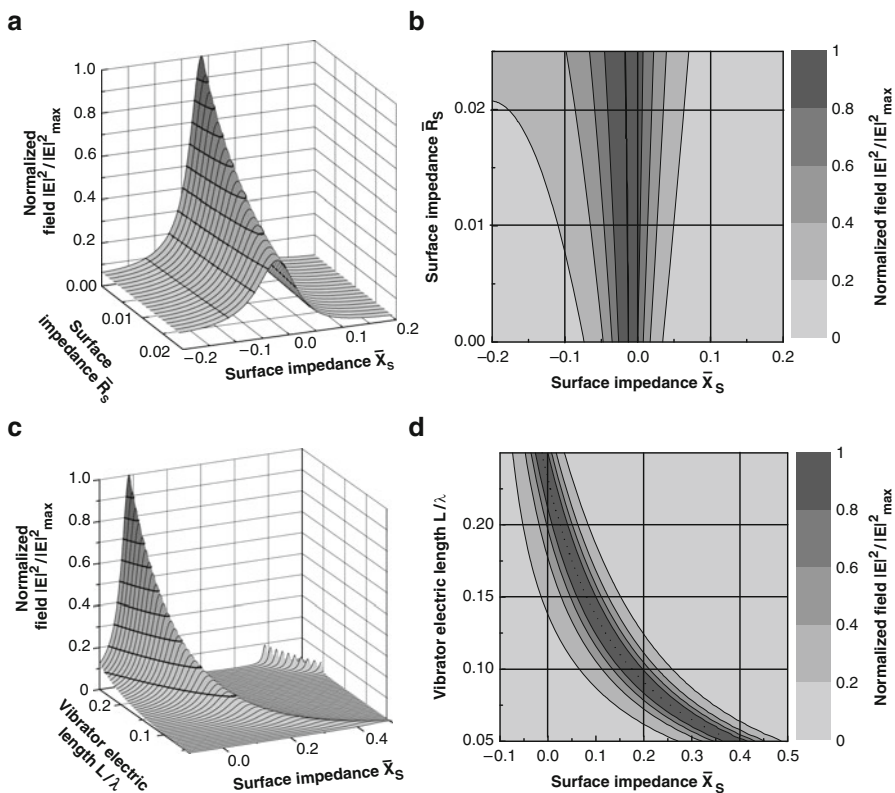


Fig. 2.19 The value of $|\bar{E}|^2$ for a vibrator in unbounded space versus active \bar{R}_S and reactive \bar{X}_S components of the surface impedance

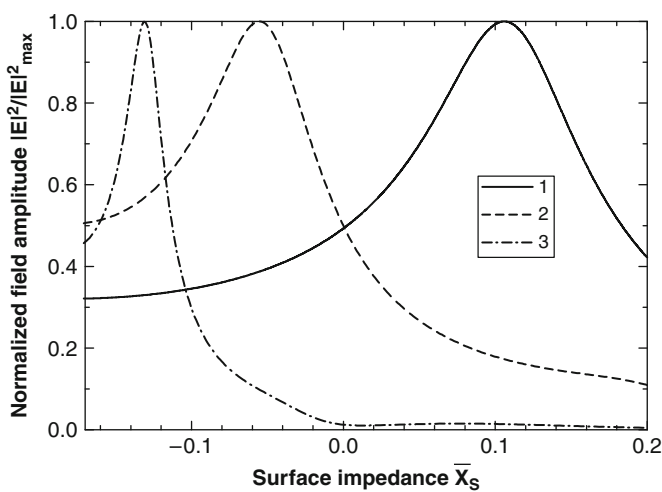


Fig. 2.20 $|\bar{E}|^2$ as a function of \bar{X}_S for a quarter-wave vibrator in different medium: 1 free space; 2 fat layer; 3 muscular tissue

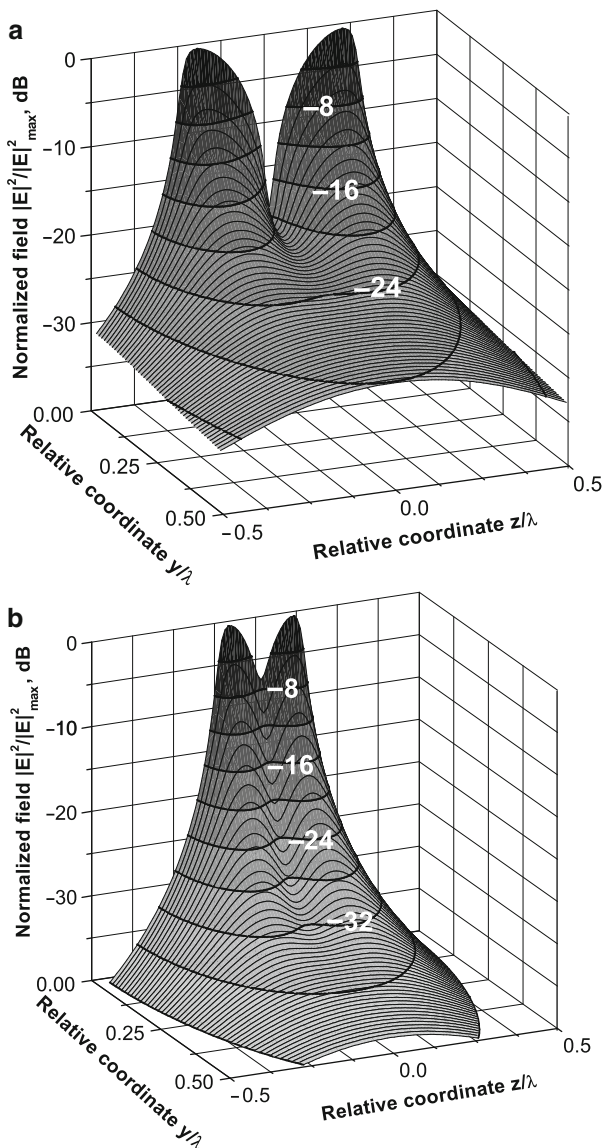


Fig. 2.21 The field distribution of a vibrator in free space: (a) $kL = \pi/2$, $\bar{X}_S = -0.013$; (b) $kL = \pi/4$, $\bar{X}_S = 0.121$

In conclusion, it may be emphasized that the model of infinite space may be applied to the analysis of impedance vibrators in real medium having finite dimensions, since excited fields in lossy medium rapidly decay as distance from the vibrator increases. A vibrator field near a metallic plane has quite different properties, and its analysis is the subject of the next chapter.

References

1. Kamke, E.: Differentialgleichungen Lösungsmethoden und Lösungen. I. Gewöhnliche Differentialgleichungen. 6. Verbesserte Auflage, Leipzig, Germany (1959) (in German).
2. Glushkovskiy, E.A., Levin, B.M., Rabinovich, E.Y.: The integral equation for the current in a thin impedance vibrator. *Radiotekhnika* **22**, 18–23 (1967) (in Russian).
3. King, R.W.P., Wu, T.: The imperfectly conducting cylindrical transmitting antenna. *IEEE Trans. Antennas Propag.* **AP-14**, 524–534 (1966).
4. Hanson, G.W.: Radiation efficiency of nano-radius dipole antennas in the microwave and far-infrared regimes. *IEEE Antennas Propag. Mag.* **50**, 66–77 (2008).
5. King, R.W.P., Scott, L.D. The cylindrical antenna as a probe for studying the electrical properties of media. *IEEE Trans. Antennas Propag.* **AP-19**, 406–416 (1971).
6. Lamensdorf, D.: An experimental investigation of dielectric-coated antennas. *IEEE Trans. Antennas Propag.* **AP-15**, 767–771 (1967).
7. Bretones, A.R., Martin, R.G., García, I.S.: Time-domain analysis of magnetic-coated wire antennas. *IEEE Trans. Antennas Propag.* **AP-43**, 591–596 (1995).
8. Miller, M.A., Talanov, V.I.: The use of the notion of the surface impedance in the theory of surface electromagnetic waves. *Izvestiya vusov USSR. Radiophysika* **4**, 795–830 (1961) (in Russian).
9. Nesterenko, M.V., Katrich, V.A.: Thin vibrators with arbitrary surface impedance as handset antennas. *Proceedings of the 5th European Personal Mobile Communications Conference*. Glasgow, Scotland, 16–20 (2003).
10. King, R.W.P., Smith, G.S.: *Antennas in Matter*. MIT Press, Cambridge, MA (1981).
11. King, R.W.P., Owens, M., Wu, T.T.: *Lateral Electromagnetic Waves*. Springer-Verlag, New York (1992).
12. Beresovskiy, V.A., Kolotilov, N.N.: *Biophysical Characteristics of a Man's Tissue*. Reference book. Naukova dumka, Kiev (1990) (in Russian).
13. Cassedy, E.S., Fainberg, J.: Back scattering cross sections of cylindrical wires of finite conductivity. *IEEE Trans. Antennas Propag.* **AP-8**, 1–7 (1960).

Thin Impedance Vibrators

Theory and Applications

Nesterenko, M.V.; Katrich, V.A.; Penkin, Y.M.; Dakhov,
V.M.; Berdnik, S.L.

2011, XIII, 107 p., Hardcover

ISBN: 978-1-4419-7849-3